LADC-1685

AECU-3072

Aerosol Collection by Wetted Fiberglas Media

ND.45612

by

Joseph A. Leary
Robert A. Clark
R. Philip Hammond
Charles S. Leopold*

48376

Contribution From
Los Alamos Scientific Laboratory
Los Alamos, New Mexico
April 28, 1954

*Philadelphia, Pennsylvania, Consultant to Los Alamos Scientific Laboratory.

56-1

Aerosol Collection by Wetted Fiberglas Media

by

Joseph A. Leary
Robert A. Clark
R. Philip Hammond
Charles S. Leopold*

ABSTRACT

A wet collection system for aerosols has been developed using fibrous media. Tests show the performance to be in accord with recently developed theory of collection by fibrous media.

The effects of varying aerosol particle size, particle density, and gas velocity have indicated that inertial impaction is the primary collection mechanism. Three-year operating experience on several full scale plant installations shows reliable performance.

*Philadelphia, Pennsylvania, Consultant to Los Alamos Scientific Laboratory.

56-2

INTRODUCTION

Theory

The collection of aerosol particles by fibrous media has been investigated by many authors.[1,2,6,9,10,11,13] Predominant collection mechanisms for such collectors are (1) direct interception, (2) diffusion, and (3) inertial impaction.

Collection by direct interception is normally considered to occur with particles of an intermediate size range.[6] For the case of laminar flow of the fluid around the collector body, the path of a given particle does not deviate from the gas streamlines. Consequently if the particle passes within a distance of $\frac{D_p}{2}$ of the collector, it will be caught. Rans[9] has deduced the following equation for the interception efficiency of a cylindrical collector:

$$(1) \qquad \eta_o \simeq \frac{1}{2.002 - \ln N_{Re}} \left[(1 + R) \ln (1 + R) - \frac{R(2 + R)}{2(1 + R)} \right]$$

Thus interception will be dependent on R, the ratio of particle diameter to the collector diameter, and on the modified Reynolds number, N_{Re}. Since N_{Re} is proportional to the gas velocity, collection by interception will also be velocity dependent except for the case $N_{Re} = 1$. For values of N_{Re} other than 1, the efficiency will increase as the velocity is increased.

The diffusional mechanism operates when a sufficiently small particle, subject to Brownian motion, describes a trajectory that is quite different from the air flow around the collector. Thus the particle has a large random displacement in the plane normal to the direction of air flow. By crossing the air flow lines the particle is subjected to the influence of the collector with a much greater probability than in Case (1). Once contact is made, the uncollected particles in the gas stream diffuse in the direction of the collector due to the concentration gradient. Langmuir[9] (10) has shown that the mean displacement of a particle subject to Brownian motion will be given by

$$(2) \qquad \bar{x}^2 = 2Dt$$

Thus the mean value of $\bar{x}^2$ increases with time, t.

The diffusion coefficient, D, is given by the Stefan-Maxwell equation

$$D = \frac{V_g}{3 \pi \eta r^2} \tag{3}$$

$$= \frac{1.99 \times 10^{-16}}{r^2} \text{ cm}^2 \text{ sec}^{-1} \text{ for air at } 750 \text{ mm Hg } 20^\circ\text{C}$$

From equations (2) and (3) it is apparent that this collection process is favored by small particles, since these have greater diffusivities than large particles. Furthermore, the efficiency will decrease as the gas velocity is increased due to the decrease in time, t, that the particle is in the proximity of the collector, which results in a smaller mean random displacement across the flow lines. An additional consequence of equation (3) is that collection by diffusion is independent of particle density.

In the case of impaction, the particle deviates from the gas stream lines because of its inertia. As the gas stream approaches the collector a sudden change in direction of flow is made around the collector. However, if the particle possesses sufficient momentum it will not follow the gas stream, but will continue to have a predominantly forward motion towards the collector. The initial particle velocity, V_o, will be reduced as the particle passes through the stationary gas in front of the collector. Langmuir[10] has shown that the stopping distance of such a particle is given by

$$X = \left[\frac{2\rho_p V_o r^2}{9\mu}\right] \left[1 + \frac{A\lambda}{r}\right] \tag{4}$$

$$= 1230\, \rho_p V_o r^2 \text{ for air at } 20^\circ\text{C}$$

Langmuir[10] has also revised Albrecht's calculations to show that a critical value of X exists at which deposition begins. Theoretically this critical value is approximately 0.27 times the fiber diameter for cylindrical collectors.

More recently,[8,13] it has been shown that the impaction efficiency is a function of the inertial parameter, ψ, and the Reynolds number only, where

(5) $$\psi = \frac{C\rho_p V_o D_p^2}{18 \mu D_c}$$

(6) $$N_{Re} = \frac{D_c V_o \rho}{\mu}$$

For geometrically and dynamically similar gas flow, the impaction efficiency will vary only with ψ.

From equations (4) and (5) it is clear that for a given collector the inertial impaction efficiency will be enhanced by large particle size, high gas velocity, and high particle density.

Application of Fibrous Media

Plant applications of fibrous media have normally been concerned with diffusional collection. Blasewitz[1] has used glass fiber beds operated at low gas velocities. Stafford and Smith have shown[11] that asbestos-base filter paper collects submicron particles with extremely high efficiencies. The original objection of low gas velocity for this type of collector has been eliminated by fabrication of deep-pleated filter sections whereby the superficial gas velocity is increased many fold. However, in many applications these filters are subject to the following disadvantages:

a. Corrosive vapors and mists cause deterioration of the filter medium, with a subsequent decrease in efficiency.
b. Pyrophoric material (such as uranium dust) has in the past ignited spontaneously with disastrous results.
c. In the case of radioactive aerosols the activity level of the filter may increase to the point where replacement and ultimate disposal present health hazards that are comparable to the original aerosol problem.

On the other hand, wet collection methods offer several operational advantages over dry filtration. Objections "a" and "b" above are unimportant in wet collection systems. Since the handling of liquid radioactive waste is today a standard effluent practice, "c" is also of secondary importance in wet collection. However, wet collection systems have been applied successfully only to large particle size ranges (> 2 microns).

We have tried to combine the advantages of wet collection with the more efficient collection by fine fibrous media. This has been accomplished by

the use of standard commercial wet-cell washer units, followed by pads constructed of fine glass fibers. Investigation of this method was begun by the authors in 1948 and was reported in a series of Atomic Energy Commission documents.[4,5] Subsequently others have investigated similar systems.[2,3]

In our work we have found that such an arrangement collects submicron particles with good efficiency. We have also demonstrated that the collection is principally by inertial impaction.

DESCRIPTION OF EQUIPMENT

A number of pilot plants and several full scale plants have been used in studying the wet-cell washer-fine fiber pad system. In all cases these units were modified commercial air washers. Figure 1 is a schematic drawing showing a basic unit consisting of wet cells, zig-zag entrainment eliminators, and a fiber pad.

The air enters the unit through the first cell that is being sprayed countercurrent to the air flow. After passing through a second bank of cells (sprayed concurrently), the air passes through the zig-zag entrainment eliminator, and thence to the fiber pad. All plants consist of multiples of the basic unit as described above. In normal arrangement two basic units operate in series.

A typical installation (Pilot Plant No. 4) is shown in Fig. 2. The construction is of galvanized iron with the interior surfaces protected with black asphaltum paint. Section (1) is the inlet air cleaning section consisting of a F.G. 25 filter followed by a Cambridge filter. Section (2) is the test aerosol injection section. The air inlet orifice (calibrated by pitot tube traverse) is at (3). Sections (4) and (5) are the washer units (manufactured by Clarage Fan Co., Kalamazoo, Michigan). Sampling points are at (6). A typical sample throat is shown in Fig. 3. Five sets of these throats were used, allowing isokinetic sampling over a range of air rates from 400 to 1000 cfm.

The full scale equipment was designed by Charles S. Leopold, Philadelphia; manufactured by the American Blower Corporation, Detroit, Michigan; utilizing Capillary cells as manufactured by Air and Refrigeration Corporation, Atlanta, Georgia.

Wet Cells

The wet cells consist of a stainless steel sheet metal frame 20 inches x 20 inches x 8 inches filled with 280-micron glass fibers to a bulk density of 4.3 lbs/cu ft. In operation each cell is continuously sprayed with approximately 9.5 gal of water per min.

Fiber Pads

The pads consist of a galvanized sheet iron frame packed with a 3/8 inch layer of glass wool (10-micron fiber diameter) to a density of 1.3 lbs/cu ft and a 1-5/8 inch layer of 280-micron glass fiber packed in a random fashion

to a density of 4.2 lbs/cu ft. The coarse fiber layer forms the upstream face of the pad. An alternate construction was tested which decreased the 280-micron fiber thickness to 1-1/8 inch, and a 1/2 inch air gap separated the fine fibers from the coarse. No difference in performance could be detected between the two types of construction. The direct contact pad was favored for the simplicity in construction and the over-all mechanical strength of the pad.[a]

Aerosol Generation

Plant production dusts and generated aerosols formed the two main sources of particulate matter used in this investigation. The generated aerosols were produced either by a pneumatic atomizer generator or a rod mill generator. The pneumatic atomizer generator is shown schematically in Fig. 4. A Spraying Systems Type 1/4 J pneumatic atomizer was used to generate droplets which were then passed through a drying section to evaporate the solution forming a dry solid particle. A moderate regulation of particle size was obtained by regulating the nozzle opening, the solution concentration and the atomizing air pressure. The rod mill generator is shown in Fig. 5. Dry material is charged into the rod mill and the aerosol is formed by passing air through the hollow shaft of the rod mill during grinding. In this generator control of particle size is possible by regulation of air rate and the thermal gradient.

---

[a] In earlier work the pads were constructed without the coarse fiber layer and with the fine fibers at lower density. The new construction had no measureable change in efficiency and improved mechanical stability.

SAMPLING AND ANALYTICAL METHODS

Sampling

Efficiency-rating samples of the feed and effluent air were taken by the method shown in Fig. 6. Interstage samples were taken to evaluate each section of the collector.

Isokinetic samples of the air were drawn continuously from the center of the duct with a sharp-edge sampling throat. The sample was passed through uniform tubing free from sharp bends to a preheater where the air was warmed to 100°F. Since most of the samples were taken from air that was saturated with water, it was necessary to reduce the relative humidity before passage through the filter paper. Samples of dry air made with and without preheating showed that this had no effect on the aerosol sample collected. Directly after being warmed, the air was passed through the filter paper at the recommended velocity of 25 ft/min. Hollingsworth-Vose No. 70 paper was used for all tests. Comparison samples collected on CWS-6 filters were in agreement with the H.V.-70 papers. The sample rate was indicated by a calibrated orifice meter; in some cases calibrated rotameters were used.

Particle-size analysis samples of the feed air were taken isokinetically in the same manner as the filter paper samples. A modified cascade impactor[12] was used in place of the filter paper sample holders. Two thicknesses of Whatmann No. 41 filter paper were used as the last stage of the impactor.

Sample Analysis

Because of the convenience and precision of counting radioactive elements, tagged compounds were used wherever possible. The various types of aerosols and generation methods are shown in Table I.

Alpha-emitting aerosol samples were counted with a flowing-methane proportional counter that was equipped with a special probe of the same dimensions as the filter paper. Beta and gamma-ray emitting samples were counted with a Geiger counter. Both instruments were calibrated each time they were used by means of standard sources. Where practical, each sample was counted long enough to give a probable error of less than 0.5%.

Collection efficiences were calculated in the following manner:

a. From the sample collection rate and collection time, the total

volume of air sampled was computed.

b. The radioactivity of each sample was divided by this total volume to give the aerosol concentration at the sample point in the duct.

c. The removal efficiency was calculated from the equation

$$\eta_T = 100 \left(1 - \frac{C_2}{C_1}\right)$$

where η_T is the per cent collected, C_1 and C_2 are the upstream and downstream aerosol concentrations, respectively.

Since the range of an alpha particle is short in paper (< 50 microns), any particles that are deeply imbedded in the paper would not be counted. This would introduce a serious error in the reported collection efficiency. In order to evaluate this, several filter papers were dissolved after counting and small aliquots of the resulting solution were radioassayed. In the six runs that were checked by this method, no significant changes in collection efficiency resulted. In the case of gamma-ray emitting aerosols this source of error does not exist, since these are highly penetrating radiations.

Particle-size analysis of the aerosol was made on each test with a modified cascade impactor that had been calibrated by S. Laskin at the University of Rochester. After counting each stage of the impactor, the mass median diameter of the aerosol was determined in the standard manner from a log-probability plot.

One source of error in using the cascade impactor is the indefiniteness of the stage E (the final filter paper stage) median diameter. This value really depends on the size distribution of the aerosol under consideration. In the case of alpha-emitting aerosols it was possible to check the size distribution on this stage by radioautograph.[7] The results of this check for seven samples are shown in Table II.

The sampling and sample analyses were checked in the following manner: All cells and pads were removed from the system, and a "tagged" $CuSO_4 \cdot 5H_2O$ aerosol was passed into the entrance chamber. Samples were collected in the standard manner. Three such "blank" runs were made, and the maximum variation of samples in a given run was always less than 2%. This indicates that sampling is reliable, and that the counting of samples is reproducible.

TEST RESULTS

The results for a single unit as defined above will be presented first on a functional basis, and later summarized by correlation of all test data in graphical form.

Particle Size

As in nearly all aerosol generation, the particle size was distributed over a reasonably large range in a given test. Consequently, each test was evaluated in terms of the mass median particle size of the aerosol. However, in the analysis of results based on this parameter, one must keep in mind the statistical nature of the aerosol. For example, in Fig. 7 we have shown a typical cascade impactor sample analysis. The value of d_g for this aerosol was 0.86 micron, and the efficiency is correlated with this size. The deviation, σ_g, of the size distribution may also be obtained from Fig. 7. From d_g, and σ_g the complete theoretical distribution can be calculated.

From Fig. 7, it is clear that in this test more than 25% by mass (approximately 93% by count) of the aerosol particles have diameters of 0.5 micron or less. Consequently, in order to collect 99% of the total mass, we must also collect these smaller particles with high efficiency. To say that an efficiency of 99% is obtained on 0.86-micron particles is of course completely erroneous. It would be desirable to determine the efficiency as a function of individual particle diameter. Preliminary analyses by radioautograph indicate an efficiency of at least 60% for a 0.3-micron particle of 7.0 g/cu cm.

In Fig. 8, the effect of d_g on efficiency is shown. The rapid approach to 100% efficiency in going from 0.5-micron to 1.0-micron median diameter is typical of impaction devices.[8,13]

Gas Velocity

A most significant variable for the classification of collection devices into mechanistic categories is the gas velocity. Whereas diffusional collection is favored by low velocity, inertial impaction improves with increasing gas velocity due to the increased aerosol particle momentum. Interception can also improve with an increase in gas velocity.

The increase in efficiency shown in Fig. 9 clearly demonstrates that diffusional collection was unimportant in these tests. This plot was constructed from individual tests. In order to extend the information to smaller particle size ranges, the efficiency values taken from the smooth curves of

Fig. 8 were cross plotted as a function of velocity in Fig. 10 for d_g = 0.8 micron and 0.7 micron. Figure 10 also demonstrates that collection by diffusion is not important in this particle size range.

Particle Density

From equations (3) and (4) it is apparent that while diffusional collectors are insensitive to particle density, an impingement device will collect low-density particles less efficiently than high-density particles, all other conditions constant. Moreover, collection by direct interception would be unaffected by variations in particle density.

In Fig. 11 we have plotted the effect of varying density on collection efficiency, when the d_g of the test aerosol was 1 micron. These results demonstrate that inertial impaction is the predominant collection mechanism for both pad and cells.

The particle size distribution of the test aerosol is changed on passing through the cells, since the larger particles are removed more efficiently. Consequently, the particle size distribution of the aerosol entering the pad will depend on the performance of the cells. The higher the removal efficiency of the cells, the smaller the d_g of the aerosol entering the pad. Since the cells are less efficient for low-density particles, the pad will receive an aerosol of a larger d_g when a low-density test aerosol is used. This will result in a higher efficiency for the pad in the low-density region. Consequently, if a correction is applied for variation in particle size, the density effect for the pad will be even greater than indicated in Fig. 11.

Component Performance

In Fig. 12 the individual efficiencies of coarse wetted cells and the 10-micron fiber pad are shown. Both components exhibit an increase in efficiency with increasing gas velocity.

Circulating Water Rate

The effect of circulating water rate was also investigated and is shown in Table III. It appears that this rate is not critical as long as the cells receive enough water to prevent channeling of the air.

Wet operation in the gas washer unit also improves the efficiency of the "dry" pad. It will be shown in the next section that the dry pad is actually covered with water droplets during wet operation. This apparently improves the collection properties somewhat.

Plant Performance

Most of the above results were obtained on the 600 cu ft/min pilot plant. In Table IV are listed all of the plant installations that have been tested to date, as well as pilot plant tests. The range of operating conditions and test aerosols for each plant are also shown.

All runs have been correlated by means of the modified impaction parameter:

$$I = \rho_p U_c D_g^2$$

For a fixed value of gas viscosity and a given collection fiber diameter, I will be directly proportional to ψ of equation (5).

In Figs. 13 and 14 the collection efficiencies of all plants tested have been plotted against I using the plotting symbols indicated in Table IV. These curves are characteristic of the upper portion of the S-shaped impaction curves obtained by Wong and Johnstone for glass fiber mats.[13] Our lowest values of I (ca. 2×10^{-6}) are equivalent to $\sqrt{\psi} \approx 1.0$ for 10-micron fibers. Wong and Johnstone have shown that the lower limit for impaction to occur is approximately $\sqrt{\psi} = 0.4$.

Pressure Drop

The pressure drops across each component as installed in the unit are plotted as a function of velocity in Figs. 15, 16, and 17. As expected, the effect of increasing the water rate on a concurrently-operated cell is slightly less than that of a countercurrent arrangement.

The pressure drop increases experienced during the first 24 months of continuous plant operation are shown in Fig. 18. The pressure drop of the first unit increased ~ 2 fold. The first Fiberglas pad section increase was not as rapid for the first 12 months (about 30%), but over a period of 24 months has increased 2 fold. Inspection of the upstream face of the first countercurrent cells showed a heavy salt deposit caused by evaporation. This deposit penetrated to a depth of 4 inches. By installing upstream spray nozzles to continuously flush the cell, this deposition was eliminated. In Fig. 19 are shown typical cells that have been operated for 9 months with, "A", and without, "B", upstream spray nozzles. Presumably it may be advantageous to operate the first bank of cells in a concurrent fashion. The countercurrent

method is used commercially for conditioning supply air to reduce plugging of the first units by very large particles. If this air has been precleaned, as is probably true for most effluent air, this precaution is unnecessary.

Test of Units as Saturators

The saturation efficiency of these units was determined by wet- and dry-bulb thermometer measurements. At a flow rate of 600 cu ft/min, and a spray rate of 9.5 gal/min/cell, the gas washer unit (2 coarse cells and zig-zag eliminator) raised the relative humidity from 58% to 90% (average of 3 tests). Identical tests with the pad installed increased the relative humidity from 58% to greater than 99% (average of 2 tests).

The pressure drop of a newly-installed dry pad normally increases by about 10% after one hour of wet operation. If the circulating water is shut off, this pressure drop will return to the original value. Fine droplets, carried over from the wet-cell section, are continuously being collected by the pad. Prolonged operation indicates that a steady-state is reached whereby the rate of droplet deposition is equal to the rates of evaporation and drainage from the pad. Thus the pad also contributes to humidification.

DISCUSSION

We have applied pilot plant experience to construct and test six individual plant installations operating at capacities of from 3,000 to 12,500 cu ft/min. The performance of these installations, operating over a wide range of variables, has been correlated with pilot plant results by means of the impaction parameter. These plants have been in continuous operation for more than three years without serious mechanical failure, prohibitive pressure drop increase or measurable changes in efficiency.

Our results are essentially in agreement with recently developed impaction theory. Ranz and Wong[9] have extended their experimental results for impaction on a single fiber to the following problem:

"A pad of 9 micron diameter glass fiber 0.5 inch thick weighs .085 lb/sq ft of surface area. For a face velocity of 120 ft/min, estimate the initial percentage penetration for 3-, 1-, and 0.3-micron particles of unit density." The solution of this problem was subjected to the following assumptions:

a. All fibers lie in planes that are normal to the direction of flow.
b. The fibers are equally spaced to give 141 layers of fibers, spaced 90 microns apart.
c. Each time the aerosol passes one layer of fibers, complete remixing occurs. Consequently if the penetration for the first layer is given by $100\ (1 - 0.1\ \eta_T)$, then for 141 layers the penetration will be given by $100\ (1 - 0.1\ \eta_T)^{141}$.

In Table V we have shown their results for $\rho_p = 1.0$, together with values for 1.0- and 0.3-micron particles of varying density that we have calculated by their method. Although these estimated efficiencies are probably higher than can be realized in practice, they indicate that collection of submicron particles by impaction is more important than has been generally realized.

Although Languir's theory of filtration[10] does not consider that impaction is operative for one-micron oleic acid particles, La Mer[6] has shown experimentally that such particles are indeed collected primarily by impaction. He has shown that inertial impaction was the principal collection mechanism for 0.7 micron diameter particles of oleic acid, stearic acid, and dioctylphthalate. All of these compounds have densities of approximately 0.8 g/cc.

Our studies were conducted in the region where N_{Re} was 0.5 for the fiber

56-15

pads and 12 for the cells. For a 1-micron particle the value of R was 0.1 for the pads and 4×10^{-3} for the cells. From equation (1) it can be shown that these values correspond to an interception efficiency of less than one per cent. This equation was derived for viscous flow conditions, while our tests were performed in the region of turbulent flow. However, the theory of interception in the turbulent flow region has not been treated adequately in the literature.

These considerations, together with the particle density effect shown in Fig. 11 indicate that aerosol collection by these gas washer units and pads is due primarily to inertial impaction.

Blasewitz, et al.,[1] have extensively investigated glass fiber beds for diffusional collection. They have shown that for particles of 0.6-micron median diameter and a density of 2.8 g/cc, the collection efficiency decreases with increasing velocity up to a superficial velocity of 50 ft/min. Above this velocity the effect is reversed, and presumably there is a change in collection mechanism from the diffusional to the inertial process. This effect was observed for all fiber arrangements tested, i.e., from 2.5-micron fibers packed to 4.0 lb/cu ft 0.25 inch deep, up to 203-micron fibers packed to 6.6 lb/cu ft 8 inches deep. Our studies of velocity effect were conducted in the range of from 55 to 236 ft/min.

Berly and his co-workers have applied our collection method to various fumes, mists, and soluble gases with the excellent results shown in Table VI.

We believe that the results presented here, corroborated by other investigators, demonstrate that this method of aerosol collection will find numerous other useful applications.

J-6-16

Nomenclature

- A = The Cunningham Factor, dimensionless
- C_1 = Upstream aerosol concentration, counts per min per cu ft
- C_2 = Downstream aerosol concentration, counts per min per cu ft
- D = Diffusion coefficient, cm^2/sec
- D_p = Diameter of aerosol particle, cm
- D_c = Diameter of cylinder, cm
- D_g = Mass median diameter of aerosol, cm
- d_g = Mass median diameter of aerosol, microns
- I = Impaction parameter, g/sec
- N_{Re} = Reynolds Number, based on the diameter of a cylinder or fiber, dimensionless
- n = Molecular concentration, molecules/cu cm
- t = Time, seconds
- U_c = Air velocity based on the superficial velocity at the face of the wet cell, cm/sec
- V_c = Air velocity based on the superficial velocity at the face of the wet cell, ft/min
- V_g = Molecular velocity, cm/sec
- V_o = The initial velocity of the particle, cm/sec
- V_p = Air velocity based on the superficial velocity at the face of the fine fiber pad, ft/min
- $\bar{x}$ = Mean displacement of a particle subject to Brownian Motion, cm
- X = Stopping distance of a particle, cm
- λ = Mean free path of an air molecule, cm
- ρ_p = Density of aerosol particle, g/cu cm
- ψ = Inertial parameter, dimensionless
- η_T = Total efficiency
- η_o = Interception efficiency
- μ = Viscosity of air, poise
- σ_g = Standard deviation of the aerosol distribution
- $R = \frac{D_p}{D_c}$
- γ = density of gas or fluid, g/cu cm

56-17

Literature Cited

(1) Blasewitz, A. G., et al., "Filtration of Radioactive Aerosols by Glass Fibers", U.S.A.E.C. Report No. HW-20847, April 16, 1951.

(2) Berly, E. M., et al., "Removal of Soluble Gases and Particulates from Air Streams", School of Public Health, Harvard University, U.S.A.E.C. Document No. NYO-1585, October 24, 1952.

(3) First, M. W., et al., "Performance of Wet Cell Washers for Aerosols", Ind. Eng. Chem., 43, No. 6, 1363-1370 (1951).

(4) Hammond, R. P., and Leary, J. A., "Decontamination of Radioactive Waste Air", Los Alamos Scientific Laboratory, U.S.A.E.C. Document No. LAMS-970, October 1949.

(5) Hammond, R. P., and Leary, J. A., in consultation with C. S. Leopold, "Air Decontamination Tests with Baffle Plate Towers, Capillary Washers, and Fiberglas Pads", U.S.A.E.C. Document No. LA-1145, September 1950.

(6) La Mer, V. K., "Studies on Filtration of Monodisperse Aerosols", Central Aerosol Laboratories, Columbia University, U.S.A.E.C. Document No. NYO-512, March 31, 1951.

(7) Leary, J. A., "Particle-Size Determination in Radioactive Aerosols by Radioautograph", Anal. Chem., 23, 850-853 (1951).

(8) Ranz, W. E., and Wong, J. B., "Impaction of Dust and Smoke Particles on Surface and Body Collectors", Ind. Eng. Chem., 44, No. 6, 1371-1380 (1952).

(9) Ranz, W. E., "I. The Role of Particle Diffusion and Interception in Aerosol Filtration", and Finn, R. K., "II. Determination of the Drag on a Cylindrical Fiber at Low Reynolds Number", Technical Report No. 8, Engineering Experiment Station, University of Illinois, January 1, 1953.

(10) Rodebush, W. H., Langmuir, I., and La Mer, V. K., "Filtration of Aerosols and the Development of Filter Materials", O.S.R.D. Report No. 865, September 4, 1942.

(11) Stafford, E., and Smith, W. J., "Dry Fibrous Air Filter Media; Performance Characteristics", Ind. Eng. Chem., 43, No. 6, 1346-1350 (1951).

(12) Voegtlin, C., and Hodge, H. C., "Pharmacology and Toxicology of Uranium Compounds", McGraw-Hill Book Company, Inc., Section 8.2, Laskin, S., 456-505 (1949).

(13) Wong, J. B., and Johnstone, H. F., "Collection of Aerosols by Fiber Mats", Technical Report No. 11, Engineering Experiment Station, University of Illinois, U.S.A.E.C. Document No. COO-1012, October 31, 1953.

56-19

ACKNOWLEDGMENT

The authors are indebted to Dr. E. R. Jette for his encouragement and advice during this work, and for his critical review of the final manuscript. Mr. James Bricker was of great assistance in the test work, especially in the analysis of data.

Table I

Summary of Aerosol Generation

Compound	Method of generation	Analytical method	ρ_p
Plant dust	Plant operation	Pu^{239} - Alpha counting	7.0
$Pu_2(C_2O_4)_3 \cdot 6H_2O$	Rod mill	Pu^{239} - Alpha counting	3.4
$LaCl_3 \cdot 7H_2O$	Pneumatic atomiser	La^{140} - Gamma counting	3.0
$CuSO_4 \cdot 5H_2O$	Rod mill	Cu^{64} - Beta counting	2.3
CuO	Rod mill	Cu^{64} - Beta counting	6.4
UO_3	Rod mill	Fluorophotometry	7.0

Table II

Mass Median Diameter
of
Stage "E" - Modified Cascade Impactor

	d_g as determined by radioautograph ρ_p = 7.0 g/cu cm
	0.46
	0.43
	0.41
	0.54
	0.51
	0.58
	0.61
Average	0.50
Laskin's calibration	0.41

5-6-21

Table III

Effect of circulating water rate on efficiency

d_E	Circulating water rate: Gallons per minute	Efficiency: 2 cells %	Pad %	Over-all %
0.93	9.8	66.2	96.2	98.7
0.92	9.8	66.3	95.7	98.5
0.91	9.8	65.6	96.1	98.6
	Average	66.0	96.0	98.6
0.95	5.1	65.9	98.1	99.4
0.93	5.1	68.5	98.0	98.9
0.96	5.1	68.8	97.7	99.3
	Average	67.7	97.9	99.2
0.93	0	54.4	94.8	97.6

56-22

Table IV

ONE UNIT

Symbol	Plant	Range of Operating Conditions V_c	d_g	ρ_p	Type of Aerosol
●	600 cfm	216	1.2 - 0.5	7.0	Insoluble plant dust Alpha-emitter
⊡	600 cfm	270	1.2 - 0.5	7.0	Insoluble plant dust Alpha-emitter
▲	600 cfm	306	1.2 - 0.5	7.0	Insoluble plant dust Alpha-emitter
⊙	600 cfm	144	1.2 - 0.5	7.0	Insoluble plant dust Alpha-emitter
⊙	600 cfm	216	1.4 - 1.0	3.4	Generated, insoluble Alpha-emitter
■	600 cfm	216	1.7 - 1.3	2.3	Generated, soluble Beta, gamma-emitter
▲	600 cfm	216	1.0 - 0.7	6.4	Generated, insoluble Beta, gamma-emitter
⊖	3000 cfm	216	2.0 - 1.3	3.0	Soluble plant dust Beta, gamma-emitter
+	3000 cfm	360	2.1 - 1.4	3.0	Soluble plant dust Beta, gamma-emitter
⊙	6000 cfm	360	0.6	3.0	Generated, soluble Beta, gamma-emitter
⊖	6000 cfm	270	0.8	3.0	Generated, soluble Beta, gamma-emitter
◐	6000 cfm	270	0.4	7.0	Insoluble plant dust Alpha-emitter
		TWO UNITS			
▬	600 cfm	252	1.1 - 0.8	7.0	Insoluble plant dust Alpha-emitter
◧	3000 cfm	216	2.3 - 1.3	3.0	Soluble plant dust Beta, gamma-emitter
◧	6000 cfm	360	0.6	3.0	Generated, soluble Beta, gamma-emitter
■	6000 cfm	270	0.8	3.0	Generated, soluble Beta, gamma-emitter

56-23.

Table V

D_p	ρ_p	Interception efficiency, η_o	$\sqrt{\psi}$	η_T	Efficiency (estimated) %
3.0	1.0	0.58	1.48	1.07	99.99
1.0	1.0	0.21	0.52	0.32	99.0
0.3	1.0	0.066	0.18	0.07	63.0
1.0	2.5	----	0.82	0.46	99.87
0.3	2.5	----	0.28	0.09	72.0
1.0	5.0	----	1.16	0.57	99.97
0.3	5.0	----	0.40	0.17	91.0
1.0	7.0	----	1.38	0.67	99.98
0.3	7.0	----	0.48	0.20	94.6

Table VI

Collection efficiencies for wetted cells and dry pads reported by Berly, et al.[2] Cells constructed of 78-micron Saran fiber.

Contaminant	d_g	Collection efficiency (one unit) %	Remarks
(1) HF gas	(1.34 mg fluoride per liter)	87.7	Pad composed of 29-micron Saran fiber plus 12-micron cotton fibers. Over-all efficiency for 2 units = 98.5%, for 3 units = 99.66%.
(2) NH_4HF_2 (mist)	4.3	> 99.9	3-micron resin bonded and 1-micron glass fibers used in place of cotton fibers. Wet stage efficiency = 97%.
(3) NH_4HF_2 (fume)	0.54	> 99.9	3-micron resin bonded and 1-micron glass fibers used in place of cotton fibers. Wet stage efficiency = 67%.
(4) $AlCl_3$ (fume)	0.59	90.3	3-micron resin bonded and 1-micron glass fibers used in place of cotton fibers. Wet stage efficiency = 67%.
(5) H_2SO_4 (mist)	4.3	98.7	3-micron resin bonded and 1-micron glass fibers used in place of cotton fibers.
(6) H_2SO_4 (mist)	0.6	83.7	3-micron resin bonded and 1-micron glass fibers used in place of cotton fibers.
(7) H_2SO_4 (mist)	0.6	96.4	3-micron resin bonded, 1-micron glass fibers and 1/2 lb of 1-micron polystyrene fibers used in place of cotton fibers.

56-25

Figure 1

Schematic Diagram of A Basic Gas Washer Unit

Figure 2

Pilot Plant For Aerosol Collection Studies

① - Air inlet

② - Aerosol inlet

③ - Orifice

④ and ⑤ - Basic gas washer units

⑥ Sample collector

Figure 3

Sample Collection Throats

Figure 4

Schematic Detail of Pneumatic Atomizer Aerosol Generator

Figure 5

Schematic Detail of Rod Mill Aerosol Generator

Figure 6

Schematic Detail of Sample Collection Unit

56-26

Figure 7

Log-Probability Plot of Cascade Impactor Data

Figure 8

Effect of d_g on Collection Efficiency of One Basic Unit
ρ_p = 7.0 g/cu cm

● = V_p = 236 ft/min
▲ = V_p = 208 ft/min
■ = V_p = 166 ft/min
▼ = V_p = 111 ft/min

Figure 9

Effect of Air Velocity on Collection Efficiency of One Basic Unit
ρ_p = 7.0 g/cu cm

● = d_g = 1.0 - 1.2 microns
▲ = d_g = 0.9 - 1.0 microns

Figure 10

Effect of Air Velocity on Collection Efficiency of One Basic Unit

Points taken from smooth curves Fig. 8. ρ_p = 7.0 g/cu cm

● = d_g = 0.8 microns
▲ = d_g = 0.7 microns

Figure 11

Effect of Particle Density on Collection Efficiency

V_p = 166 ft/min, d_g = 1.0 microns

● = One basic unit

▲ = Fine fiber pad

■ = Two wet cells

Figure 12

Effect of Air Velocity on Collection Efficiency

ρ_p = 7.0 g/cu cm

d_g = 1.0 ± 0.1 microns

● = One basic unit

▲ = Fine fiber pad

■ = Two wet cells

Figure 13

Performance Curve for One Basic Unit

Symbols from Table IV

Figure 14

Performance Curve for Two Basic Units in Series

Symbols from Table IV

Figure 15

Effect of Air Velocity on Pressure Drop in A Countercurrent Wet Cell

Fiber diameter = 280 microns

Packing density = 4.3 lb/cu ft

● = Spray rate = 9 gpm ▲ = Spray rate = 7 gpm ■ = Spray rate = 0 gpm

Figure 16

Effect of Air Velocity on Pressure Drop in a Concurrent Wet Cell

Fiber diameter = 280 microns

Packing density = 4.3 lb/cu ft

● = Spray rate = 9 gpm

▲ = Spray rate = 7 gpm

■ = Spray rate = 0 gpm

Figure 17

Effect of Air Velocity on Pressure Drop in a Fine Fiber Pad

Fiber diameter = 10 microns

Packing density = 1.3 lb/cu ft

Figure 18

Effect of Continuous Operation on Pressure Drop

● = First basic unit, two wet cells in series (before installation of upstream spray nozzles)

V_c = 166 ft/min

Packing density = 4.3 lb/cu ft

▲ = First unit, fine fiber pads

V_p = 125 ft/min

Packing density = 1.3 lb/cu ft

■ = Second unit, two wet cells in series

V_c = 166 ft/min

Packing density = 4.3 lb/cu ft

▼ = Second unit, fine fiber pads

V_p = 125 ft/min

Packing density = 1.3 lb/cu ft

Figure 19

Countercurrent Wet Cells After Nine Months' Continuous Operation in First Unit (Upstream Face)

A - After upstream spray nozzle installation

B - Before upstream spray nozzle installation

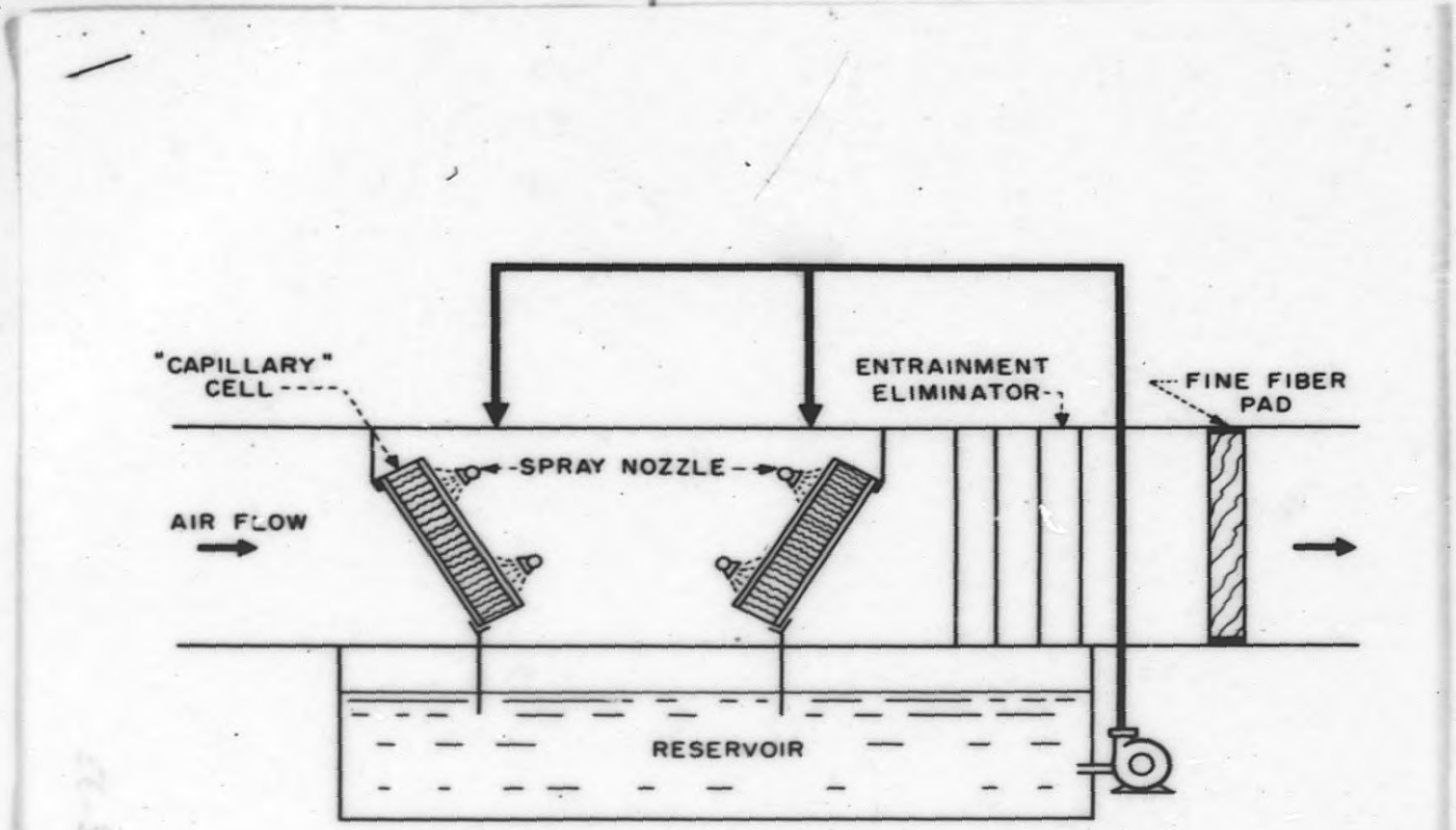

Figure 1

Schematic Diagram of A Basic Gas Washer Unit

56-31

Figure 2

Pilot Plant For Aerosol Collection Studies

① - Air inlet

② - Aerosol inlet

③ - Orifice

④ and ⑤ - Basic gas washer units

⑥ Sample collector

56-33

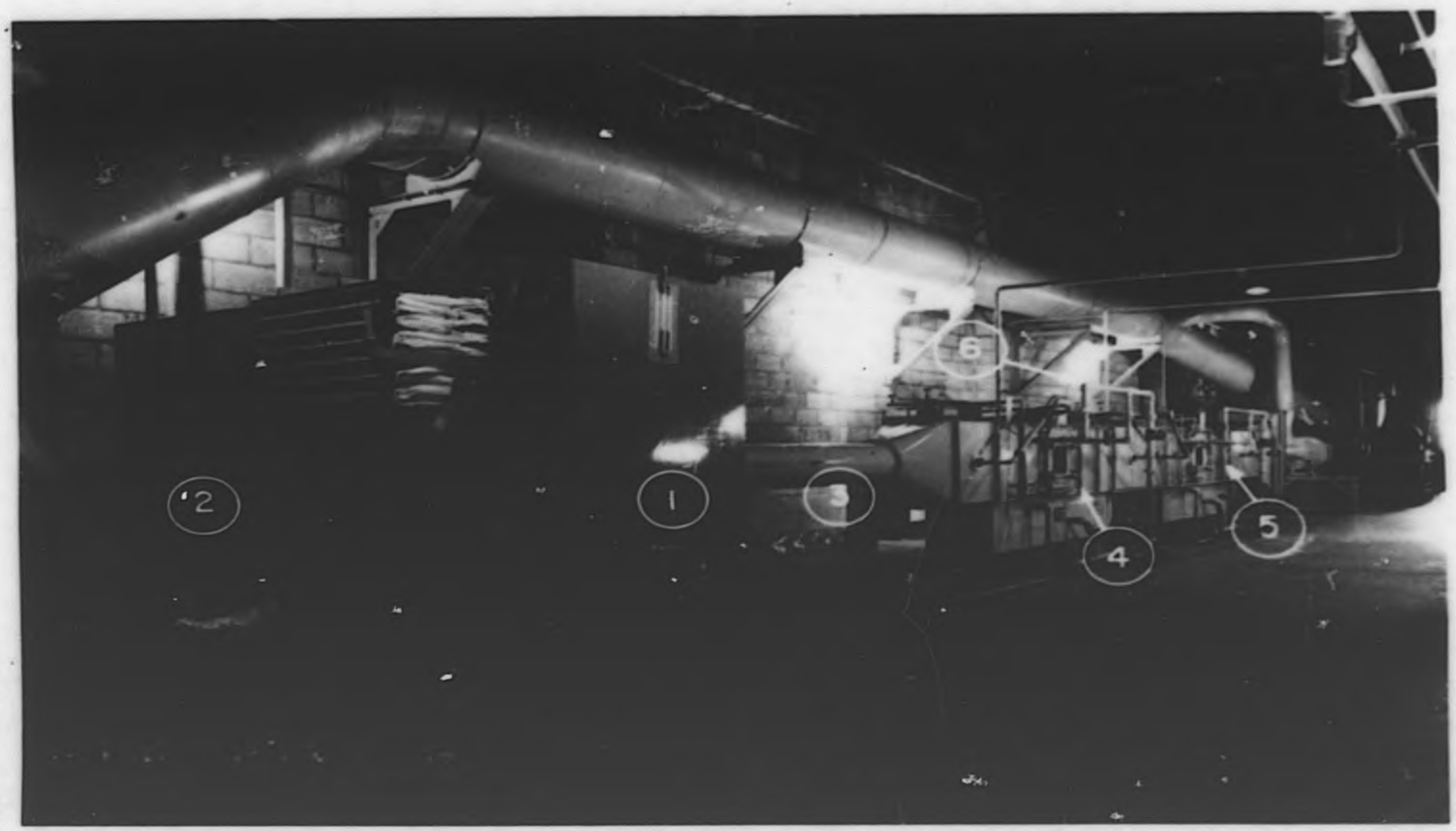

56-34

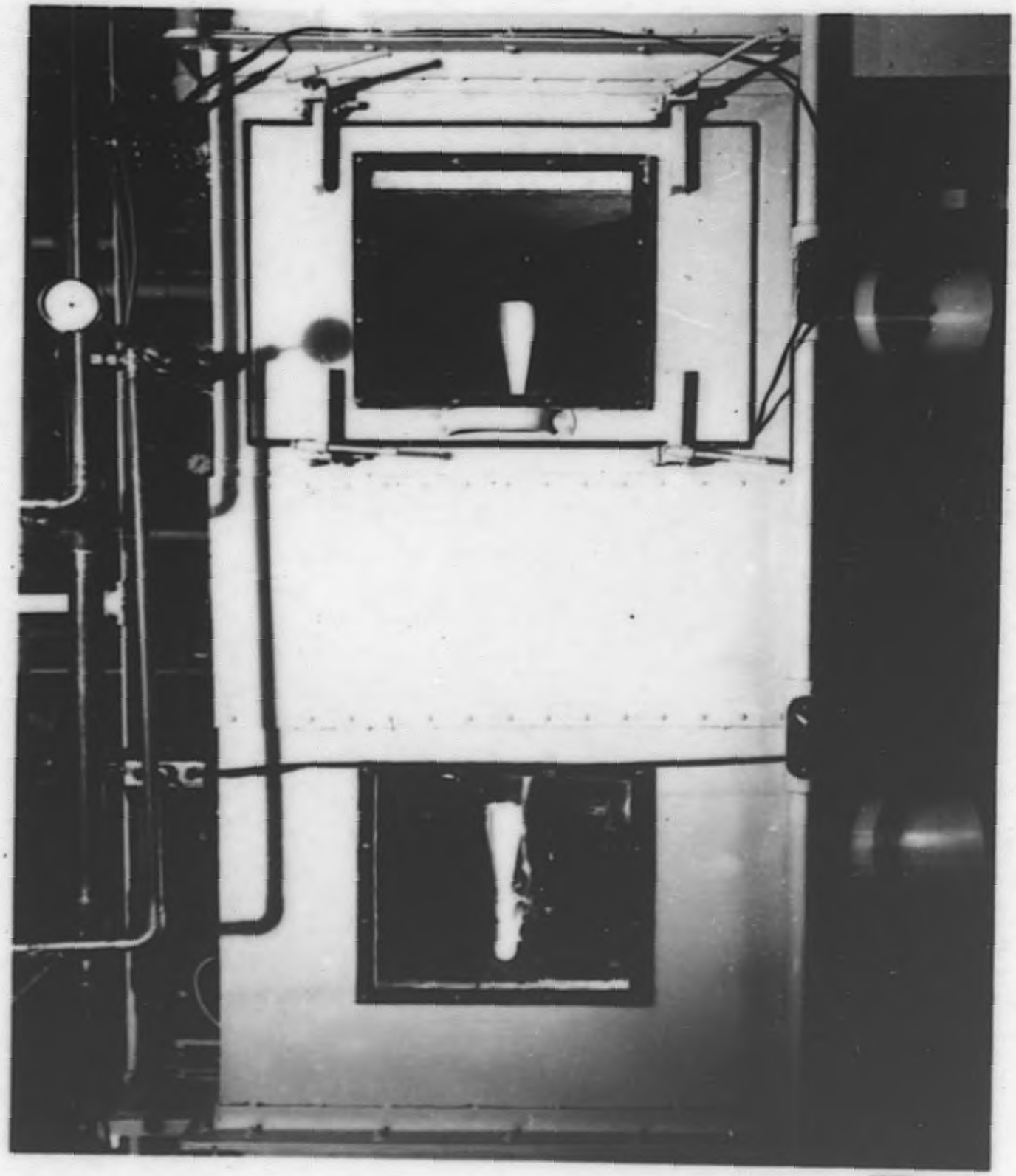

FL-36

Figure 3

Sample Collection Throats

56-35

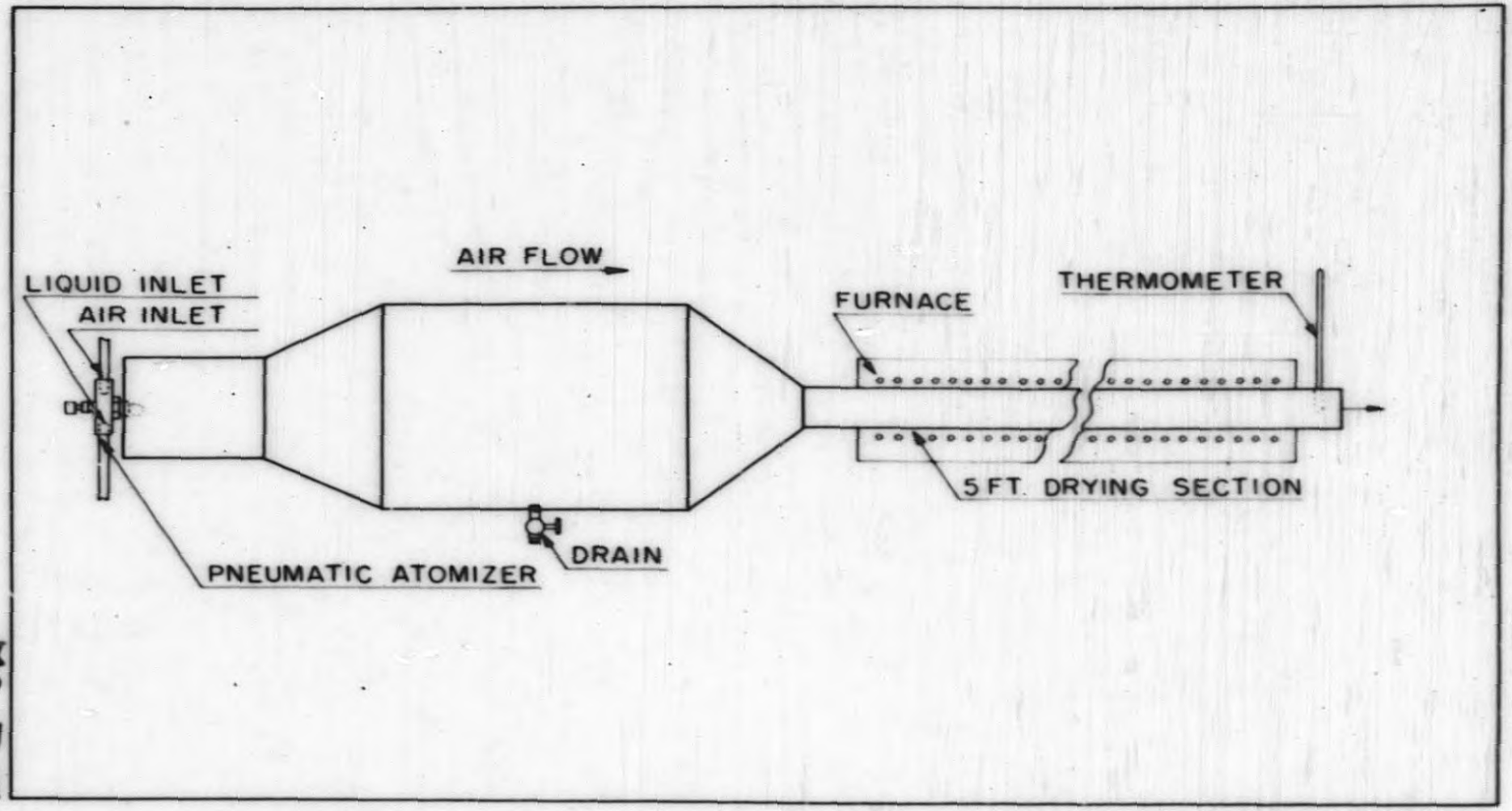

86-95

Figure 4

Schematic Detail of Pneumatic Atomizer Aerosol Generator

56-37

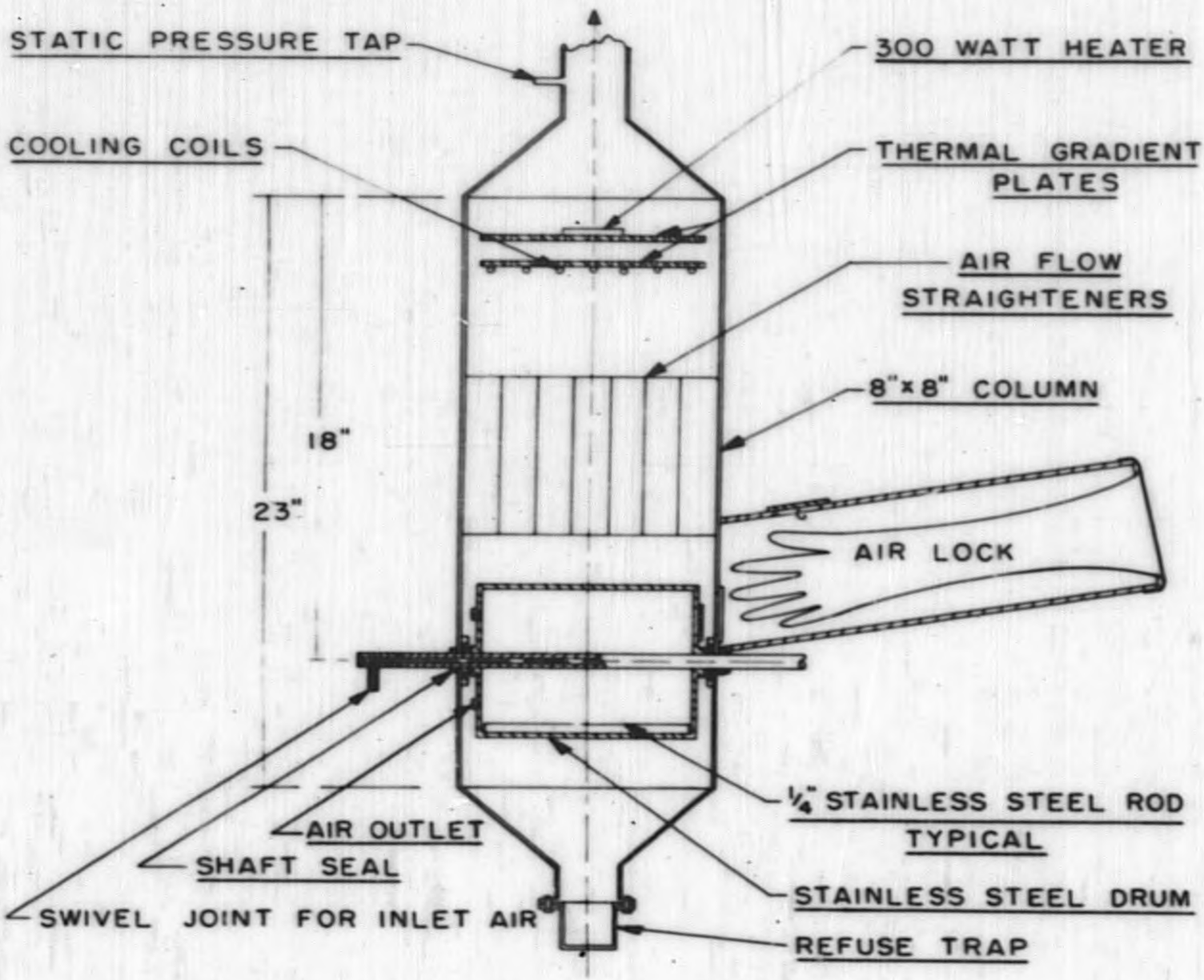

Figure 5

Schematic Detail of Rod Mill Aerosol Generator

56-39

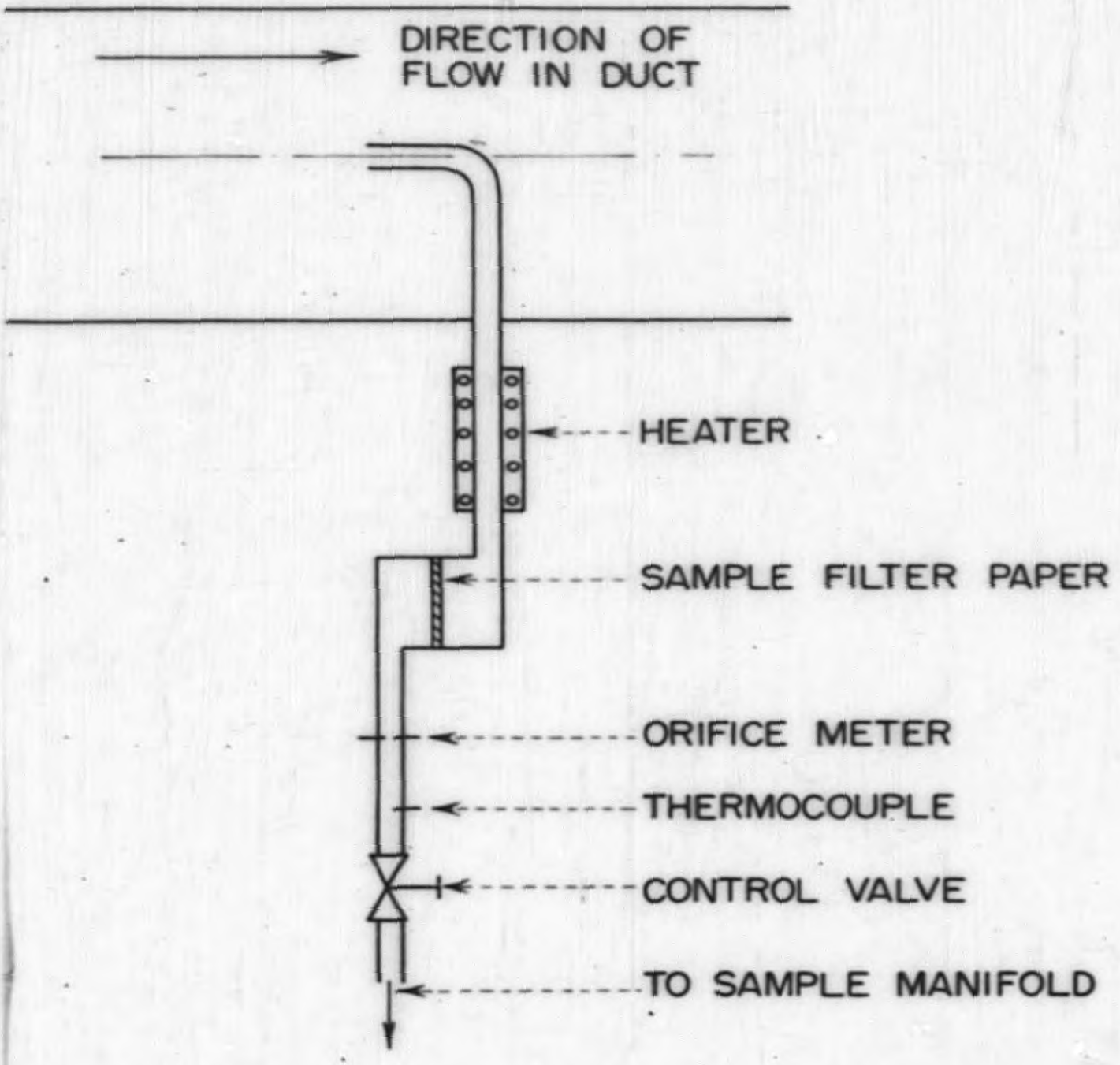

Figure 6

Schematic Detail of Sample Collection Unit

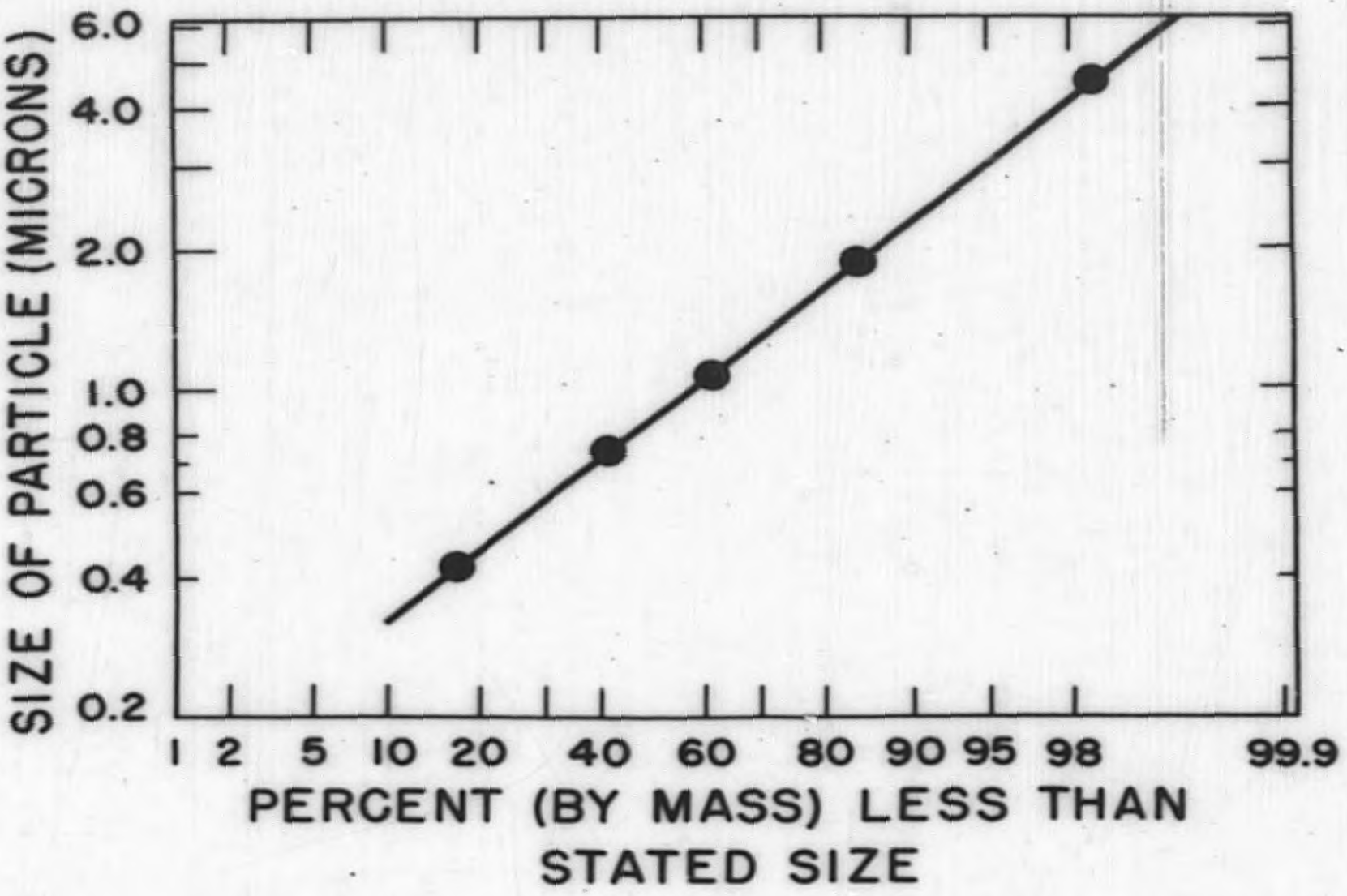

Figure 7

Log-Probability Plot of Cascade Impactor Data

56-43

56-44

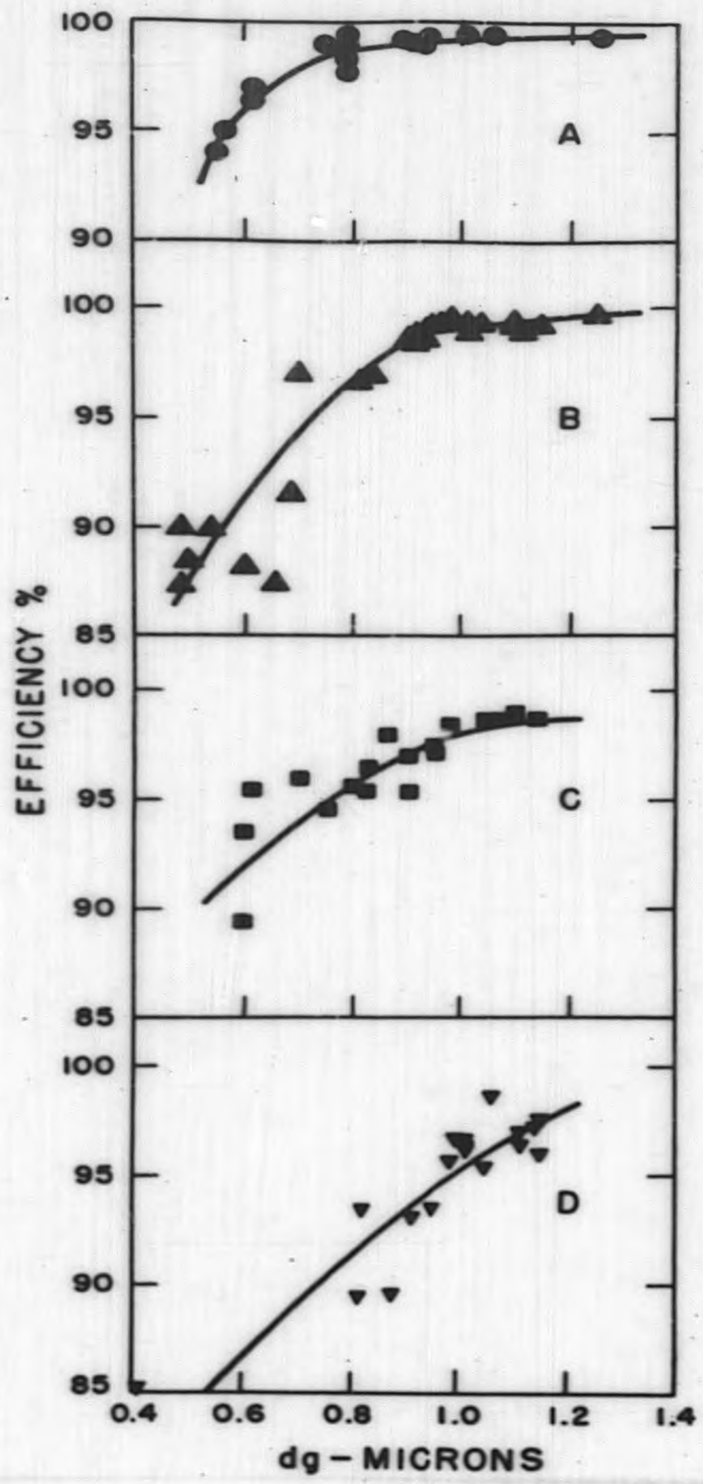

56-46

Figure 8

Effect of d_g on Collection Efficiency of One Basic Unit

ρ_p = 7.0 g/cu cm

● - V_p = 236 ft/min

▲ - V_p = 208 ft/min

■ - V_p = 166 ft/min

▼ - V_p = 111 ft/min

56-45

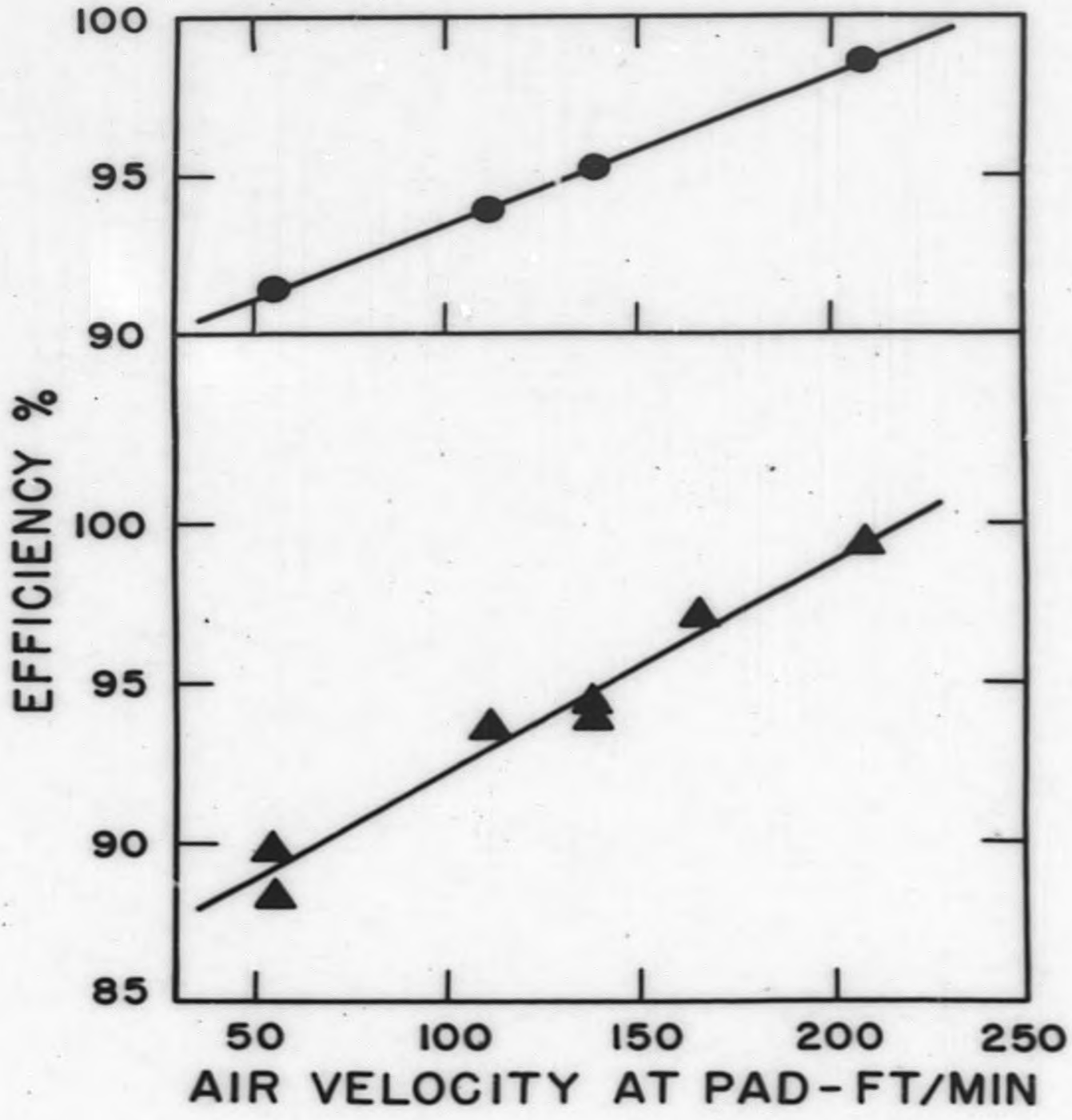

56-48

Figure 9

Effect of Air Velocity on Collection Efficiency of One Basic Unit
ρ_p = 7.0 g/cu cm

● - d_g = 1.0 - 1.2 microns

▲ - d_g = 0.9 - 1.0 microns

56-47

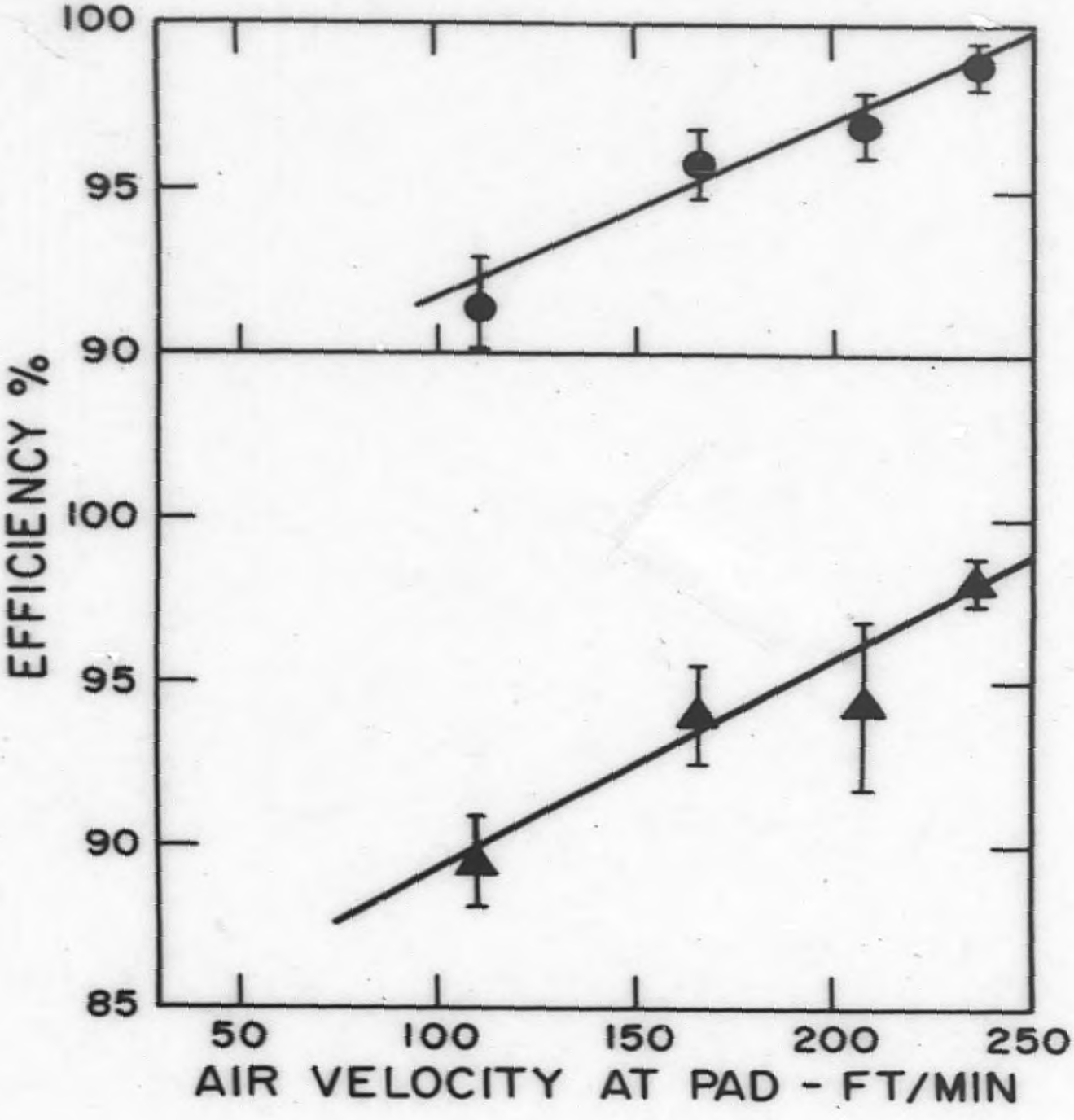

56-50

Figure 10

Effect of Air Velocity on Collection Efficiency of One Basic Unit

Points taken from smooth curves Fig. 8. ρ_p = 7.0 g/cu cm

● - d_g = 0.8 microns

▲ - d_g = 0.7 microns

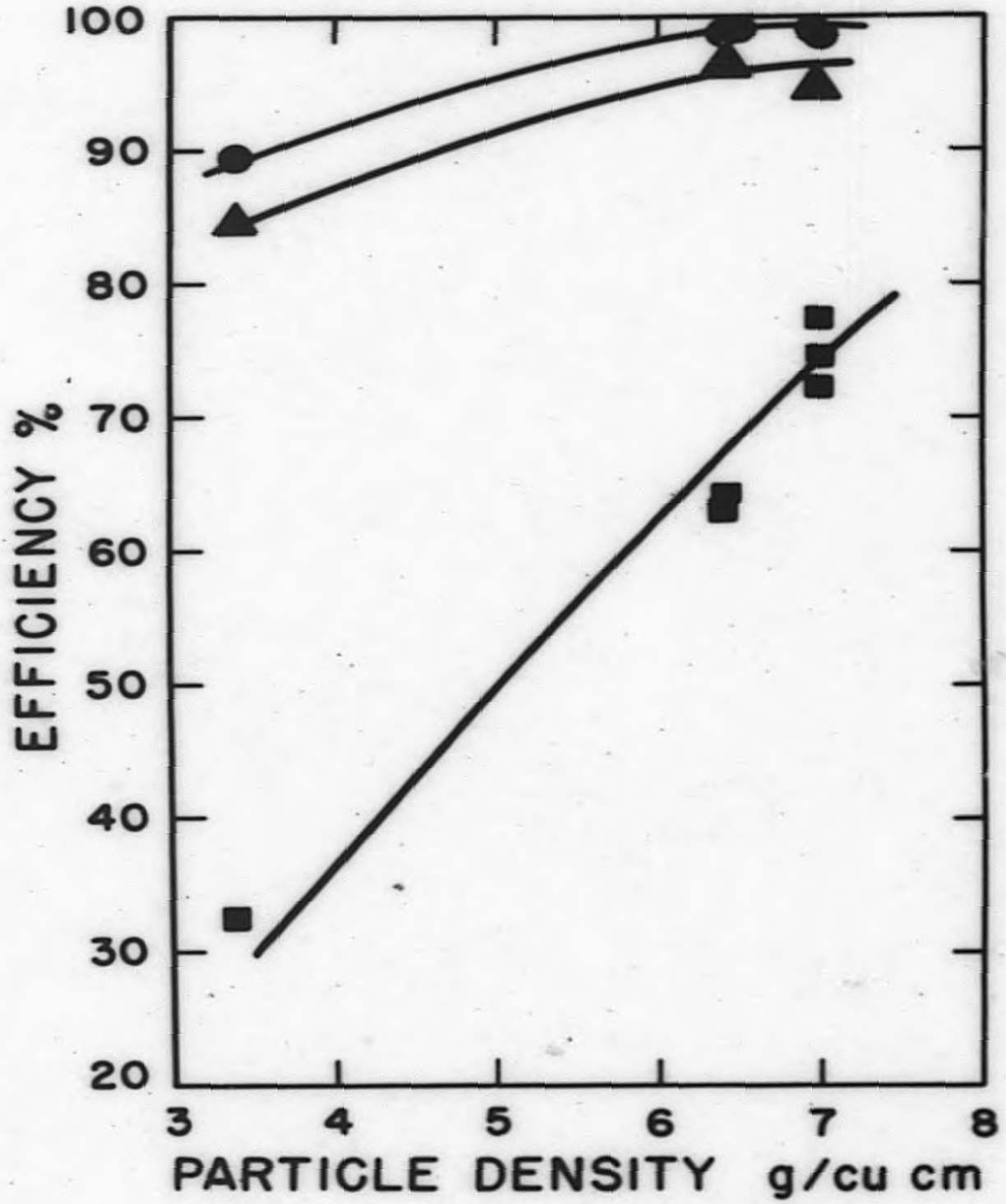

Figure 11

Effect of Particle Density on Collection Efficiency

V_p = 166 ft/min, d_g = 1.0 microns

● = One basic unit

▲ = Fine fiber pad

■ = Two wet cells

56-51

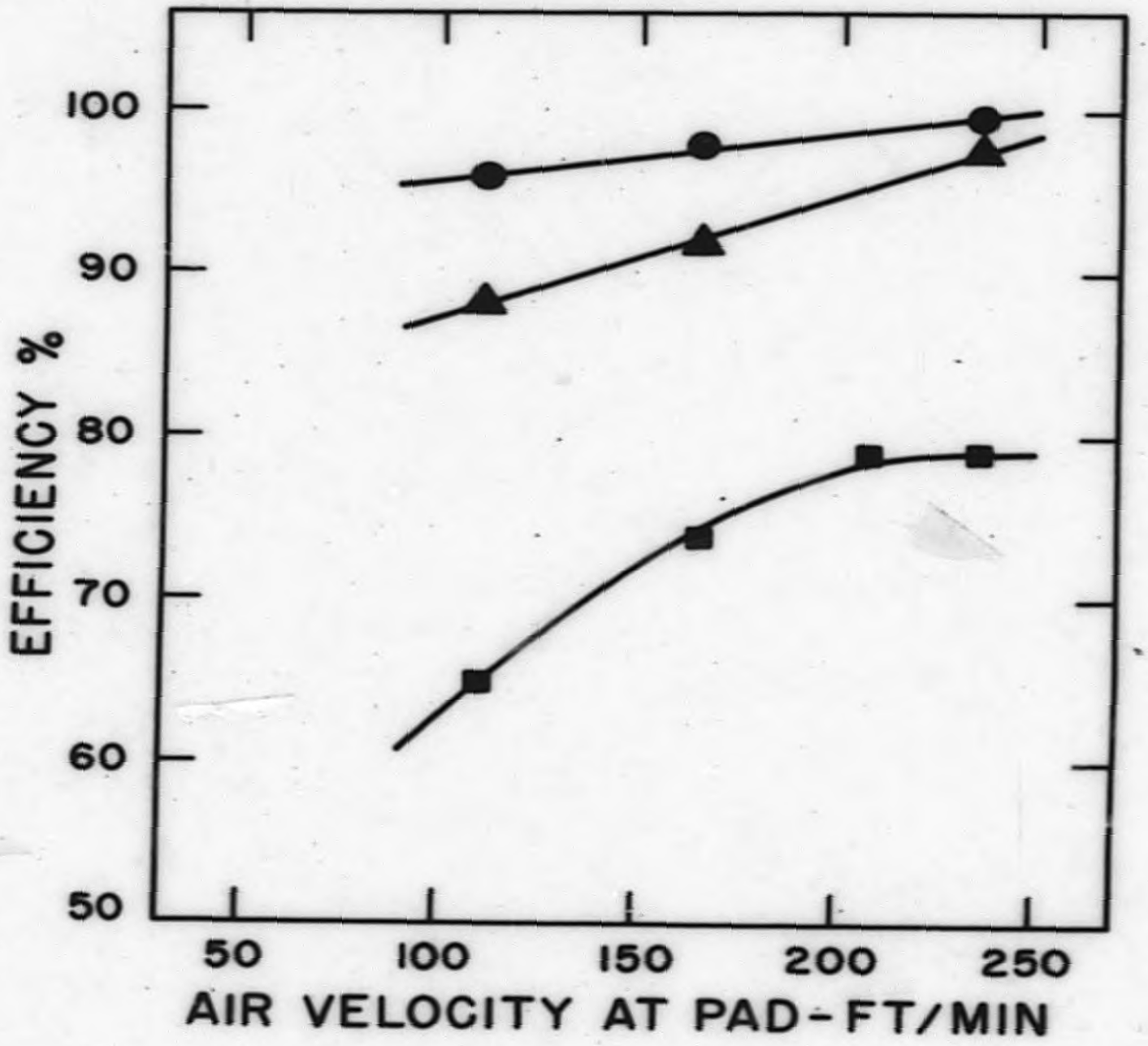

56-54

Figure 12

Effect of Air Velocity on Collection Efficiency

ρ_p = 7.0 g/cu cm

d_g = 1.0 ± 0.1 microns

● - One basic unit

▲ - Fine fiber pad

■ - Two wet cells

56-58

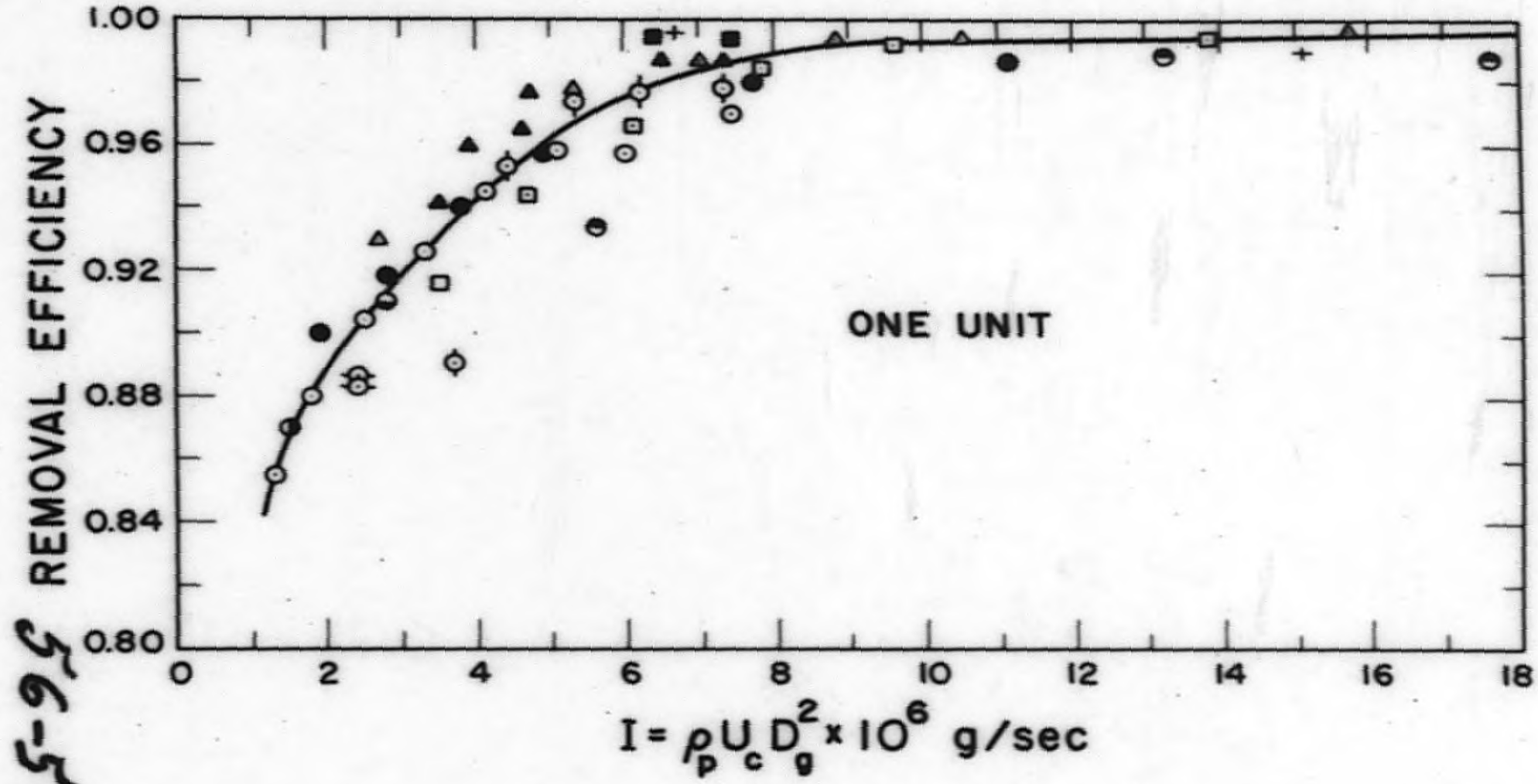

Figure 13

Performance Curve for One Basic Unit

Symbols from Table IV

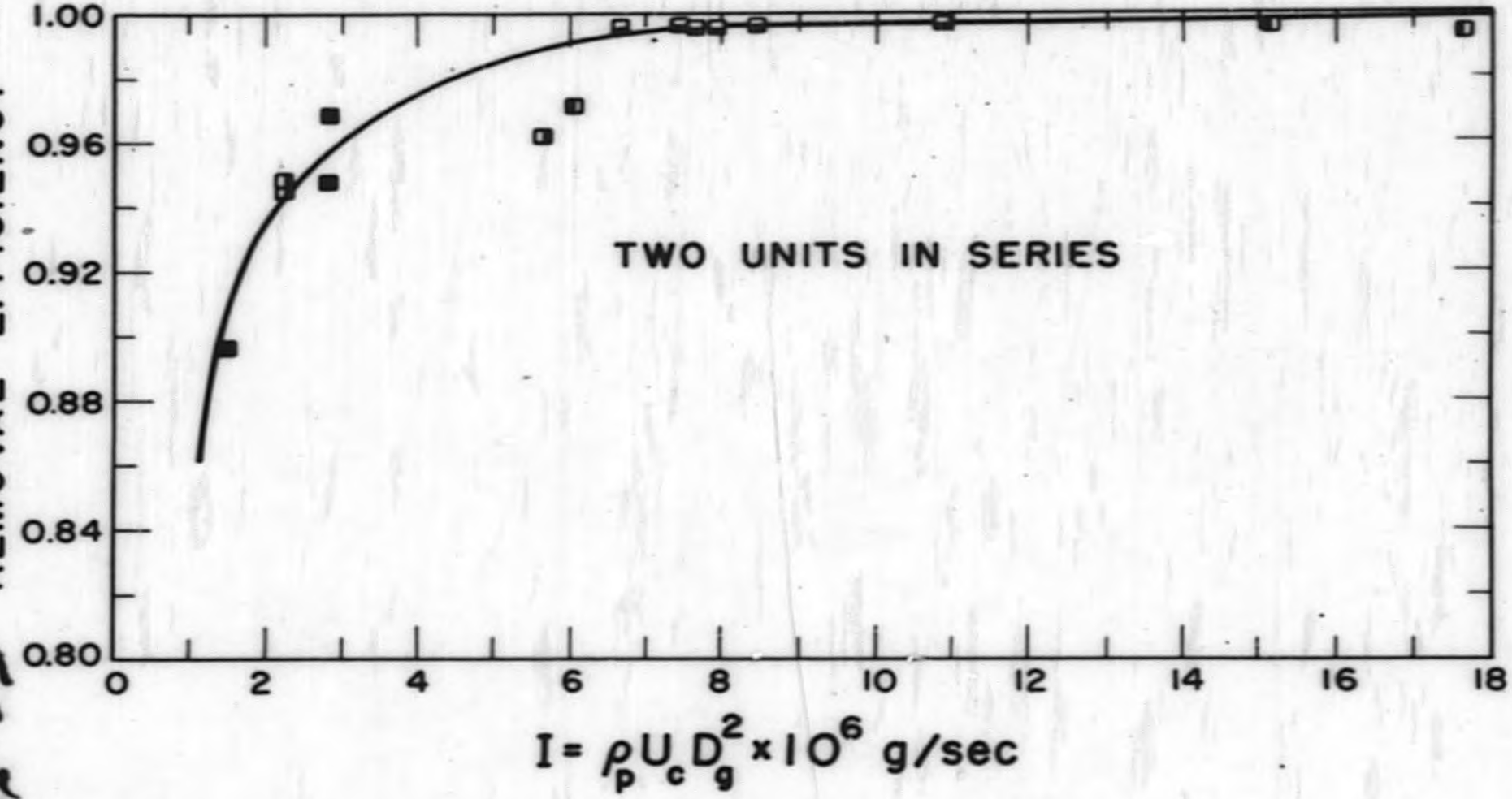

BG-95

Figure 14

Performance Curve for Two Basic Units in Series

Symbols from Table IV

56-57

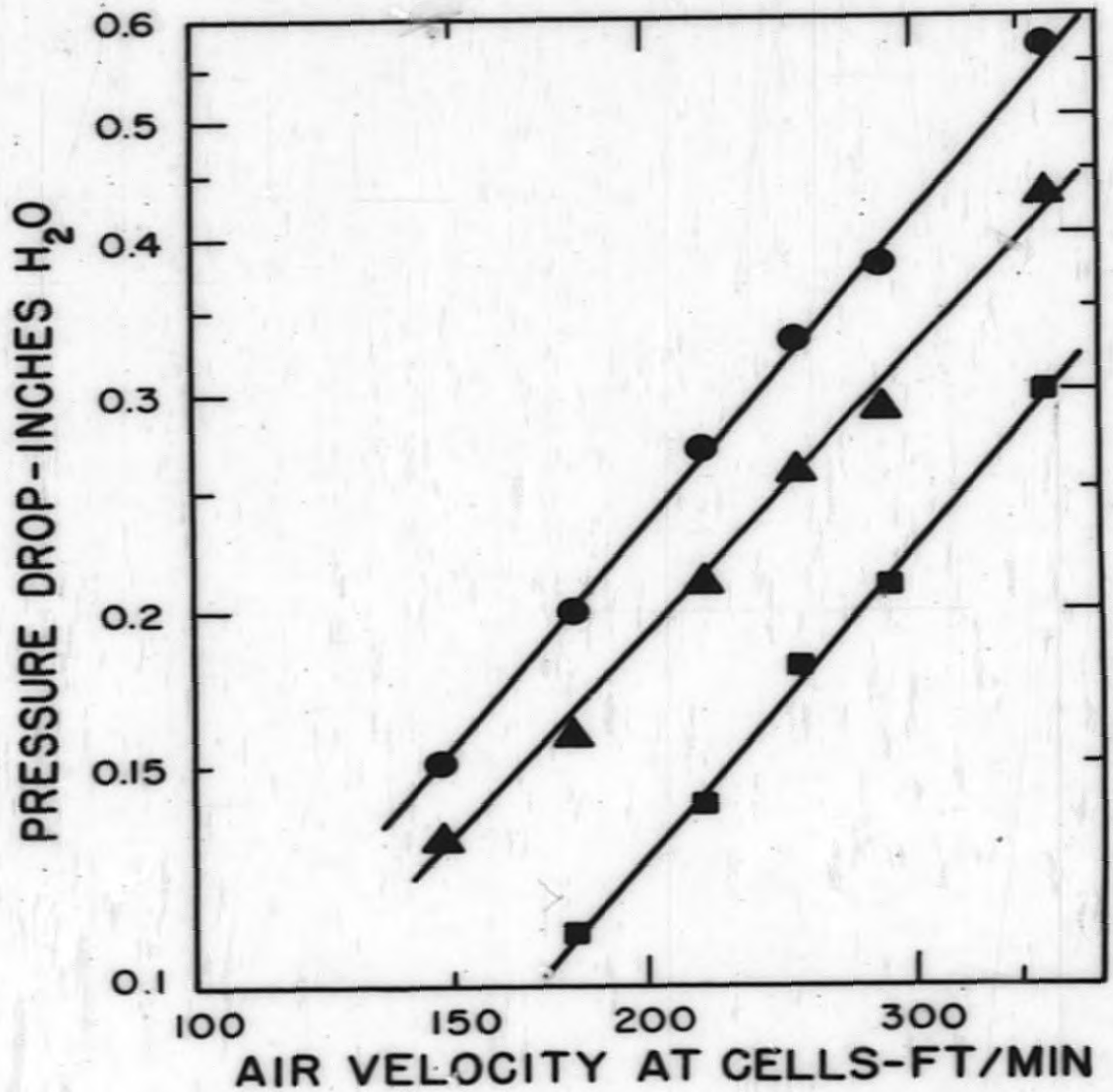

56-60

Figure 15

Effect of Air Velocity on Pressure Drop in A Countercurrent Wet Cell

Fiber diameter = 280 microns

Packing density = 4.3 lb/cu ft

● = Spray rate = 9 gpm ▲ = Spray rate = 7 gpm ■ = Spray rate = 0 gpm

56-59

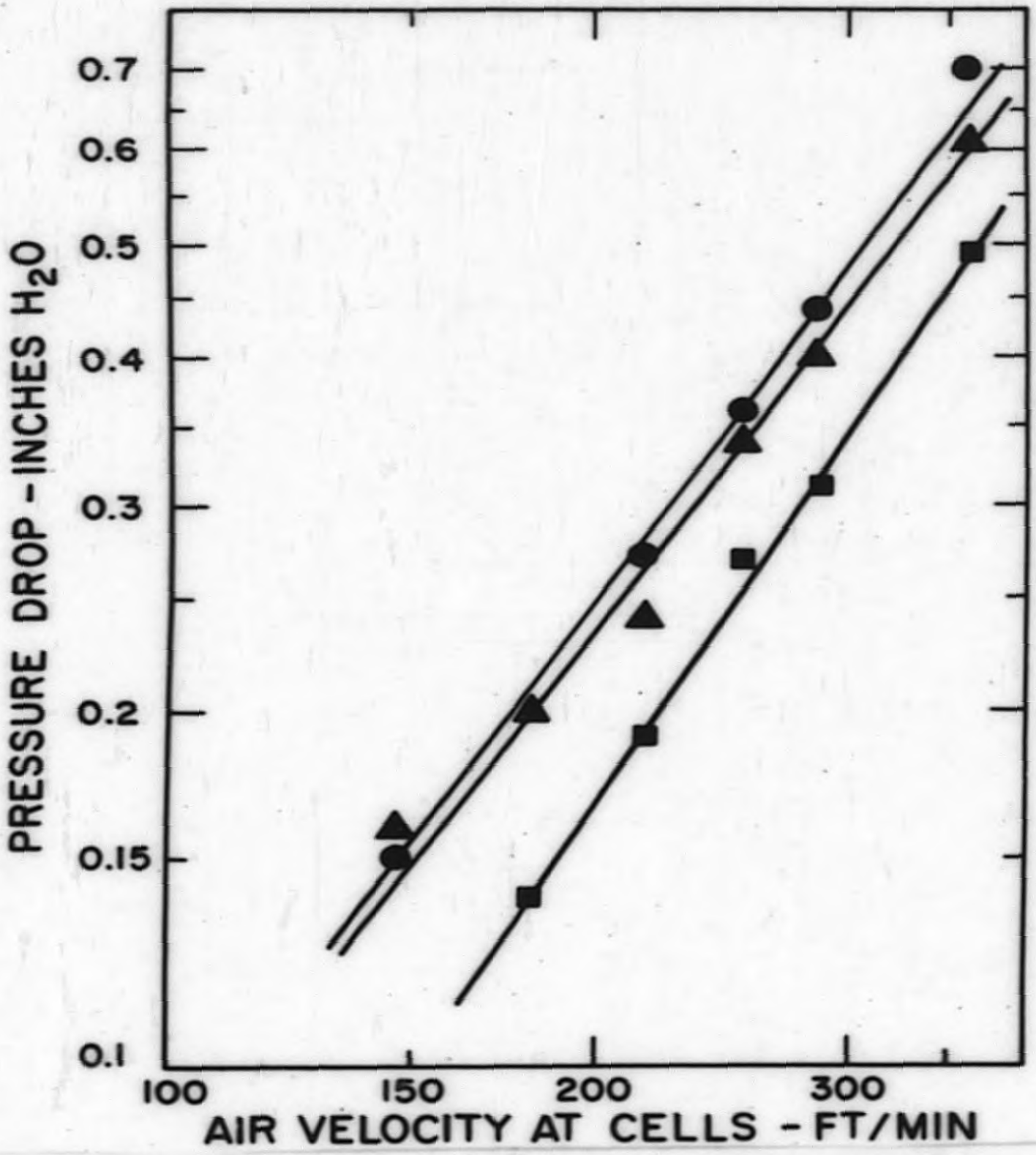

Figure 16

Effect of Air Velocity on Pressure Drop in a Concurrent Wet Cell

Fiber diameter = 280 microns

Packing density = 4.3 lb/cu ft

● = Spray rate = 9 gpm

▲ = Spray rate = 7 gpm

■ = Spray rate = 0 gpm

56-61

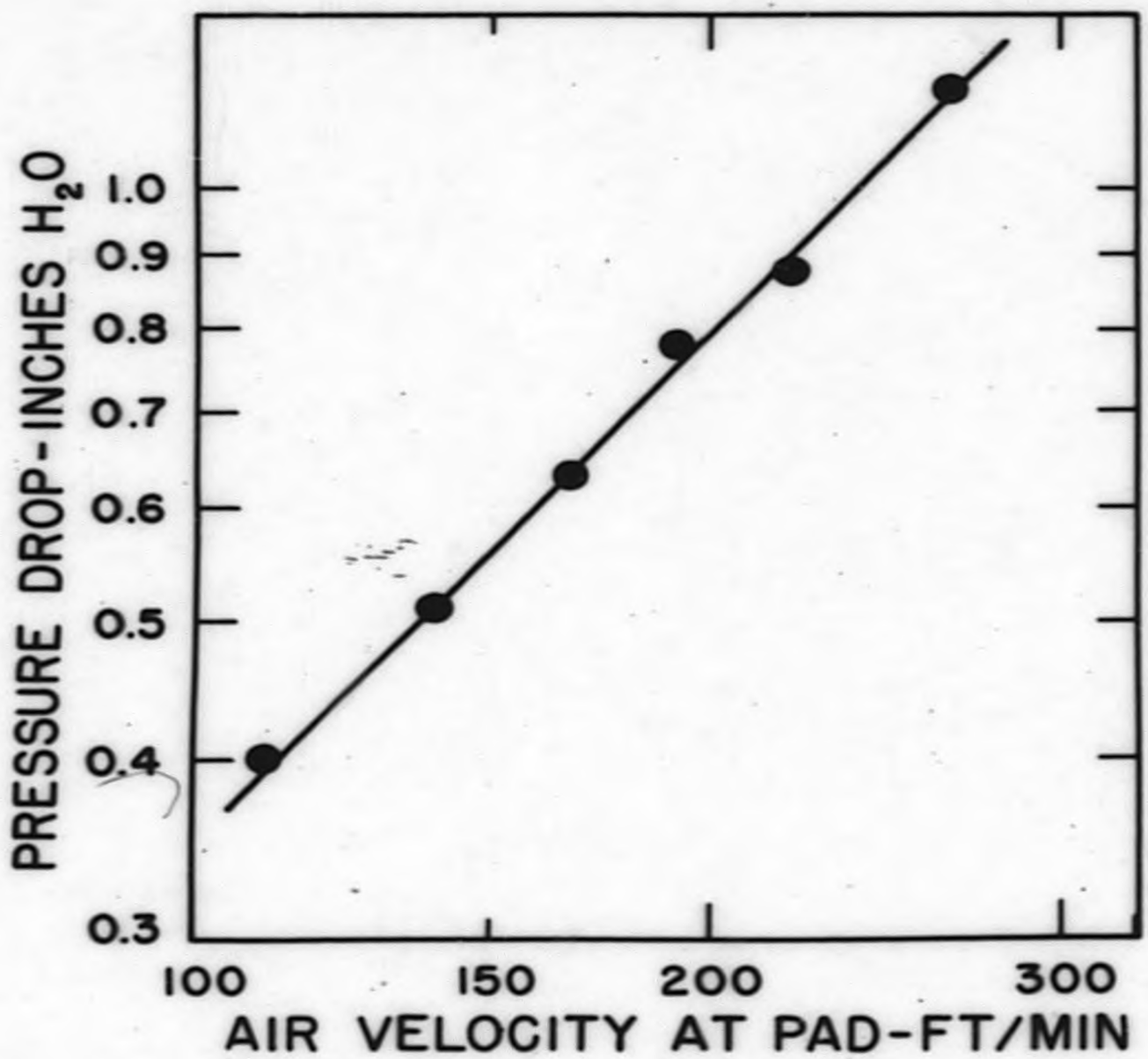

Figure 17

Effect of Air Velocity on Pressure Drop in a Fine Fiber Pad

Fiber diameter = 10 microns

Packing density = 1.3 lb/cu ft

56-63

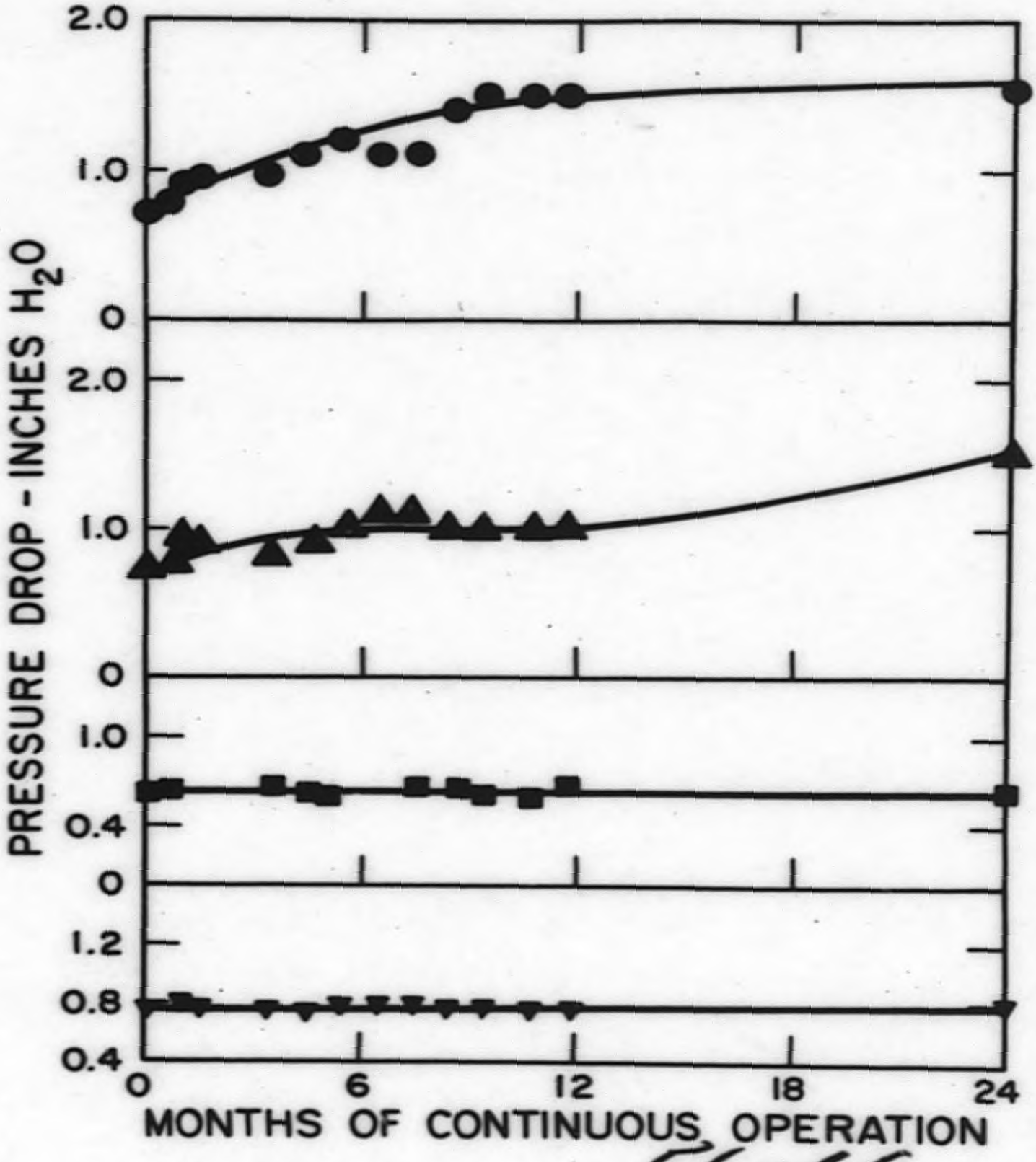
2.0
1.0
0
2.0
1.0
0
1.0
0.4
0
1.2
0.8
0.4
PRESSURE DROP - INCHES H_2O
0
6
12
18
24
MONTHS OF CONTINUOUS OPERATION

56-66

Figure 18

Effect of Continuous Operation on Pressure Drop

● = First basic unit, two wet cells in series (before installation of upstream spray nozzles)

V_c = 166 ft/min

Packing density = 4.3 lb/cu ft

▲ = First unit, fine fiber pads

V_p = 125 ft/min

Packing density = 1.3 lb/cu ft

■ = Second unit, two wet cells in series

V_c = 166 ft/min

Packing density = 4.3 lb/cu ft

▼ = Second unit, fine fiber pads

V_p = 125 ft/min

Packing density = 1.3 lb/cu ft

56-65

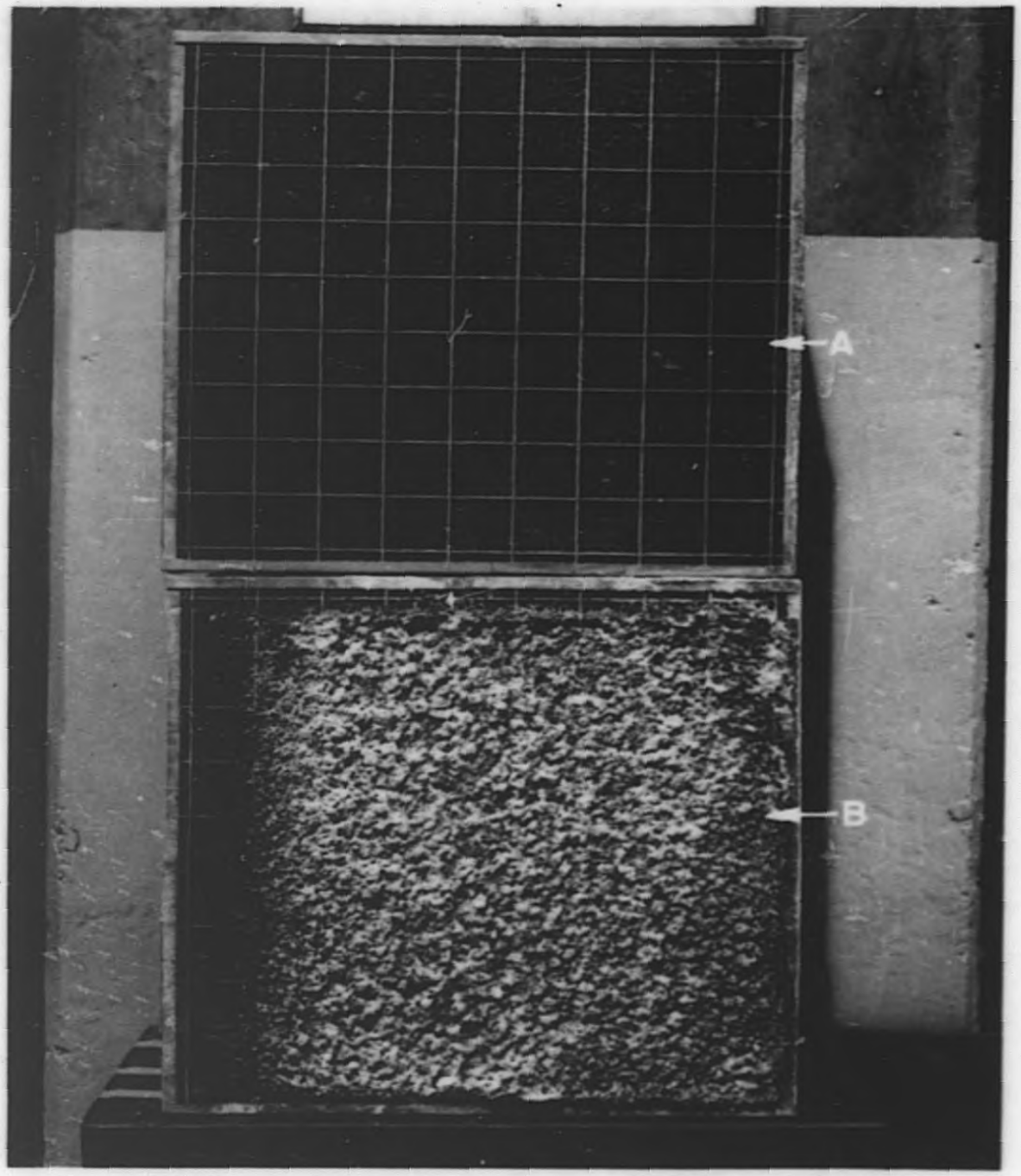

56-68

Figure 19

Countercurrent Wet Cells After Nine Months' Continuous Operation in First Unit (Upstream Face)

A - After upstream spray nozzle installation

B - Before upstream spray nozzle installation

56-67

END